

RECEIVED: March 3, 2024

ACCEPTED: June 25, 2024

PUBLISHED: July 16, 2024

Search for dark QCD with emerging jets in proton-proton collisions at $\sqrt{s} = 13 \text{ TeV}$



The CMS collaboration

E-mail: cms-publication-committee-chair@cern.ch

ABSTRACT: A search for “emerging jets” produced in proton-proton collisions at a center-of-mass energy of 13 TeV is performed using data collected by the CMS experiment corresponding to an integrated luminosity of 138 fb^{-1} . This search examines a hypothetical dark quantum chromodynamics (QCD) sector that couples to the standard model (SM) through a scalar mediator. The scalar mediator decays into an SM quark and a dark sector quark. As the dark sector quark showers and hadronizes, it produces long-lived dark mesons that subsequently decay into SM particles, resulting in a jet, known as an emerging jet, with multiple displaced vertices. This search looks for pair production of the scalar mediator at the LHC, which yields events with two SM jets and two emerging jets at leading order. The results are interpreted using two dark sector models with different flavor structures, and exclude mediator masses up to 1950 (1950) GeV for an unflavored (flavor-aligned) dark QCD model. The unflavored results surpass a previous search for emerging jets by setting the most stringent mediator mass exclusion limits to date, while the flavor-aligned results provide the first direct mediator mass exclusion limits to date.

KEYWORDS: Beyond Standard Model, Dark Matter, Hadron-Hadron Scattering, Jets

ARXIV EPRINT: [2403.01556](https://arxiv.org/abs/2403.01556)

JHEP07(2024)142

Contents

1	Introduction	1
2	The CMS detector	3
3	Event simulation	4
4	Event reconstruction and triggering	5
5	Analysis	7
5.1	Event and physics object selection	7
5.2	EJ tagging	8
5.3	Determining the EJ tagging and event selection criteria	12
6	Background estimation	12
6.1	Validation tests	16
7	Systematic uncertainties	17
7.1	Background uncertainties	17
7.2	Signal uncertainties	19
8	Results	20
9	Summary	24
The CMS collaboration		30

1 Introduction

Although there is a preponderance of evidence from astronomical and cosmological observations [1–5] for the existence of dark matter (DM), it has not yet been detected in laboratories, suggesting that its origin may be associated with as-of-yet unobserved physics processes beyond the standard model (SM). As experimental searches have excluded a large portion of the phase space of DM models with weakly interacting massive particles, alternative theoretical models have been developed with a hidden gauge sector, some of which are similar to quantum chromodynamics (QCD), which can result in strongly self-interacting DM particles [6–9]. Dark matter of this type could interact with SM particles through so-called mediator particles and potentially be produced at colliders, generating signatures such as semivisible jets [10] or emerging jets (EJs) [11].

The search described in this paper is motivated by the models proposed in refs. [11–13]. A composite dark sector with a QCD-like non-Abelian gauge symmetry $SU(N_{\text{color}}^{\text{dark}})$, where $N_{\text{color}}^{\text{dark}}$ is the number of dark colors, is added to the SM gauge group. We consider the case where fermions in the dark sector (dark quarks Q_{dark}) interact with the SM quarks

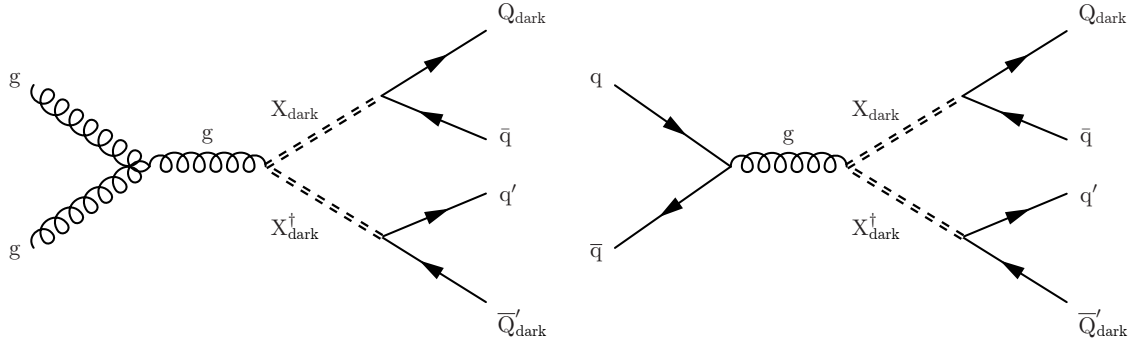


Figure 1. Feynman diagrams for pair production of dark mediator particles via gluon-gluon fusion (left) and quark-antiquark annihilation (right), with each mediator decaying to an SM quark and a dark quark.

through a scalar mediator X_{dark} . The scalar mediator is charged under both SM QCD and dark QCD and couples to a quark and a dark quark via Yukawa interactions with coupling strength $\kappa_{\alpha i}$, where the subscript α (i) denotes flavors of dark (SM) quarks. The mediator can be pair produced through gluon splitting at the LHC, similar to the pair production of a single type of squark in supersymmetry [14]. In fact, the production cross section is the same as for pair production of right-handed top squarks [15, 16] multiplied by $N_{\text{color}}^{\text{dark}}$. Each mediator decays into a quark and a dark quark, as shown in figure 1. The dark quarks hadronize into dark hadrons. Generally, of the dark hadrons in the composite QCD-like dark sector described above, either the lightest dark baryon or dark meson is stable and thus provides a natural DM candidate.

The first version of this model that we consider, referred to as “unflavored”, has a simplified flavor structure in the coupling of the dark sector to SM particles, such that only the Yukawa coupling to the d quark is nonnegligible [11]. Equation (1.1), taken from ref. [11], gives the proper decay length of dark pions in this model:

$$c\tau_{\pi_{\text{dark}}} = 80 \text{ mm} \left(\frac{1}{\kappa^4} \right) \left(\frac{2 \text{ GeV}}{f_{\pi_{\text{dark}}}} \right)^2 \left(\frac{100 \text{ MeV}}{m_d} \right)^2 \left(\frac{2 \text{ GeV}}{m_{\pi_{\text{dark}}}} \right) \left(\frac{m_{X_{\text{dark}}}}{1 \text{ TeV}} \right)^4, \quad (1.1)$$

where κ is the coupling between dark quarks and the SM down quark, $f_{\pi_{\text{dark}}}$ is the dark pion decay constant, m_d is the mass of the SM down quark, and $m_{\pi_{\text{dark}}}$ is the dark pion mass. The numbers with units show the expected typical scale for each variable.

If instead multiple Yukawa couplings $\kappa_{\alpha i}$ have nonnegligible values, the proper decay length for dark mesons composed of dark quarks of flavor indices α and β is given by eq. (1.2) from ref. [13]:

$$c\tau_{\pi_{\text{dark}}}^{\alpha\beta} = \frac{8\pi m_{X_{\text{dark}}}^4 c\hbar}{N_c m_{\pi_{\text{dark}}} f_{\pi_{\text{dark}}}^2 \sum_{i,j} |\kappa_{\alpha i} \kappa_{\beta j}^*|^2 (m_i^2 + m_j^2) \sqrt{\left(1 - \frac{(m_i + m_j)^2}{m_{\pi_{\text{dark}}}^2}\right) \left(1 - \frac{(m_i - m_j)^2}{m_{\pi_{\text{dark}}}^2}\right)}}, \quad (1.2)$$

where $m_{X_{\text{dark}}}$ is the mediator particle mass, N_c is the SM color factor, and m_i, m_j are the masses of the SM quarks with flavor indices i, j , respectively. Within this model, we focus

on the “flavor-aligned” scenario from ref. [13], which has three dark quark flavors that couple to the SM down-type quarks (d , s , b) via a diagonal matrix $\kappa_{\alpha i} = \kappa_0 \delta_{\alpha i}$. Because of spin considerations, dark hadron decays to heavier SM particles are favored, typically resulting in a large number of b quarks in the decays when kinematically allowed. We characterize the flavor-aligned model in terms of the maximum proper lifetime for any dark pion, $c\tau_{\pi_{\text{dark}}}^{\text{max}}$. Following the benchmark models from refs. [11, 13], where the lightest dark baryon is stable, and given that dark baryon production is suppressed by $1/N_{\text{color}}^{\text{dark}}$ [17], we consider only dark meson production and require all dark mesons to decay finally into SM particles. When the lifetimes are long enough to give macroscopic decay distances, the resulting signature from either model is two SM jets and two EJs containing multiple displaced vertices.

Previous experimental searches for strongly self-interacting DM have been made using proton-proton (pp) collision data collected at the CERN LHC at $\sqrt{s} = 13$ TeV and corresponding to about 140 fb^{-1} . This includes a search for semivisible jets by the CMS Collaboration [18], a search for semivisible jets by the ATLAS Collaboration [19], and a search for dark quarks in a dijet final state by ATLAS [20]. In addition, a previous search for EJs interpreted with an unflavored dark sector model was performed by the CMS Collaboration using a data sample collected in 2016, corresponding to an integrated luminosity of 16.1 fb^{-1} [21].

In this paper, we present a search for the EJ signatures of the unflavored and the flavor-aligned dark sector models, focusing on the displacement information of the tracks in the EJ, using the data set collected by the CMS Collaboration in 2016–2018 using pp collisions at a center-of-mass energy of 13 TeV and corresponding to 138 fb^{-1} . The search strategy first identifies EJs by exploiting their topological differences relative to SM jets using selection criteria optimized separately for each model. Then, the probability for an SM jet to be misidentified as an EJ is measured, and the background is estimated using control samples in data. The main background comes from SM multijet production where SM jets are misidentified as EJs.

Compared to the previous analysis [21], we have extended the unflavored EJ model search to a wider parameter space. This study also includes the first dedicated search for a flavored dark QCD sector. We have implemented a number of important changes that considerably increase the sensitivity of the search, including the incorporation of a machine learning (ML) technique aimed at enhancing the EJ identification (tagging) performance. The tabulated results are provided as a HEPData record [22].

This paper is organized as follows. In section 2 we give an introduction of the CMS detector, followed in section 3 by a detailed description of the simulated data used in this search. The event reconstruction and triggering algorithms are discussed in section 4. In section 5 we present the analysis strategy and two independent EJ tagging methods. section 6 describes the background estimation method. The treatment of uncertainties is detailed in section 7. The results are presented in section 8 and summarized in section 9.

2 The CMS detector

The central feature of the CMS apparatus is a superconducting solenoid of 6 m internal diameter, providing a magnetic field of 3.8 T. Located within the solenoid volume are a silicon pixel and strip tracker, a lead tungstate crystal electromagnetic calorimeter (ECAL),

and a brass and scintillator hadron calorimeter (HCAL), each composed of a barrel and two endcap sections. Forward calorimeters extend the pseudorapidity (η) coverage provided by the barrel and endcap detectors. Muons are measured in gas-ionization detectors embedded in the steel flux-return yoke outside the solenoid.

The silicon tracker used in 2016 measured charged particles within the range $|\eta| < 2.5$. For nonisolated particles of $1 < p_T < 10 \text{ GeV}$ and $|\eta| < 1.4$, the track resolutions were typically 1.5% in p_T and 25–90 (45–150) μm in the transverse (longitudinal) impact parameter d_{xy} (d_z) [23]. At the start of 2017, a new pixel detector was installed [24]; the upgraded tracker measured particles up to $|\eta| < 3.0$ with typical resolutions of 1.5% in p_T and 20–75 μm in d_{xy} for nonisolated particles of $1 < p_T < 10 \text{ GeV}$ [25].

Physics events of interest are selected using a two-tiered trigger system. The first level, called the level-1 trigger, is composed of custom hardware processors and uses information from the calorimeters and muon detectors to select events at a rate of around 100 kHz within a fixed latency of about 4 μs [26]. The second level, known as the high-level trigger, consists of a farm of processors running a version of the full event reconstruction software optimized for fast processing, and reduces the event rate to around 1 kHz before data storage [27]. A more detailed description of the CMS detector, together with a definition of the coordinate system used and the relevant kinematic variables, can be found in ref. [28].

3 Event simulation

Monte Carlo (MC) events are used to evaluate the signal acceptance, optimize selection criteria, and test the closure of the background estimation methods.

The signal process is generated using the Hidden Valley module [29, 30] in PYTHIA version 8.240 [31], based on ref. [11]. In the unflavored scenario, we choose the number of dark quark flavors to be $N_{\text{flavor}}^{\text{dark}} = 7$, following ref. [11]. The running of the dark coupling constant with Q^2 , where Q is the momentum transfer, is faster for smaller $N_{\text{flavor}}^{\text{dark}}$, and the resulting showers have fewer dark mesons. In the flavor-aligned scenario, $N_{\text{flavor}}^{\text{dark}} = 3$ is used, and $\kappa_{\alpha i}$ is set to be diagonal, with all diagonal elements having the value κ_0 . For this scenario, the PYTHIA Hidden Valley module is modified to produce the different dark hadron species at the desired occurrence frequencies based on the dark quark flavors. For both cases, we consider a representation similar to QCD with $N_{\text{color}}^{\text{dark}} = 3$. The dark quark masses are degenerate and equal to the confinement scale Λ_{dark} . The dark pion mass is set to be half of Λ_{dark} , and the dark ρ meson mass four times the dark pion mass. These parameter choices are motivated by the assumptions made concerning dark matter energy density and energy scales in ref. [11]. The natural width of X_{dark} is set to 10 GeV, a relatively small value compared to the detector resolution. Under these assumptions, the free parameters of the model are limited to the mediator mass $m_{X_{\text{dark}}}$, the dark pion mass $m_{\pi_{\text{dark}}}$, and the dark pion lifetime $c\tau_{\pi_{\text{dark}}}$. Tables 1 and 2 summarize the signal model parameters used in this search. The signal cross section, described in section 1, is computed at next-to-leading order (NLO), with the resummation of soft gluon emission included at next-to-leading-logarithmic accuracy.

We simulate SM QCD multijet events and $\gamma + \text{jets}$ events using the MADGRAPH5_aMC@NLO 2.6.5 event generator [32] at leading order with the MLM matching procedure [33].

Model parameter	List of values
$m_{X_{\text{dark}}}$ [GeV]	1000, 1200, 1400, 1500, 1600, 1800, 2000, 2200, 2400, 2500
$m_{\pi_{\text{dark}}}$ [GeV]	10, 20
$c\tau_{\pi_{\text{dark}}}$ [mm]	1, 2, 5, 25, 45, 60, 100, 150, 225, 300, 500, 1000

Table 1. Model parameters for the unflavored model.

In all cases parton showering and hadronization is performed using PYTHIA8 with the CP5 underlying event tune [34] and the NNPDF3.1 next-to-NLO parton distribution functions (PDFs) [35]. The response of the CMS detector is modeled using GEANT4 [36], and corrections are applied to the simulated samples to account for the differences in resolutions and efficiencies between the data and the simulation.

4 Event reconstruction and triggering

A global “particle-flow” (PF) algorithm [37] aims to reconstruct all individual particles in an event, combining information provided by the tracker, calorimeters, and muon system. The reconstructed information from the different subsystems is used to build physics objects such as photons, leptons, jets, and missing transverse momentum [38–40].

The pp interaction vertices are reconstructed by clustering tracks on the basis of their z coordinates along the beamline at their points of closest approach to the beam axis using a deterministic annealing algorithm [41]. The position of each vertex is estimated with an adaptive vertex fit [42].

Multiple vertex candidates can be reconstructed because of additional pp interactions in a bunch crossing (pileup). The primary vertex (PV) is taken to be the vertex corresponding to the hardest scattering in the event, evaluated using tracking information alone, as described in section 9.4.1 of ref. [43]. The contribution from charged-particle tracks from pileup interactions is reduced by rejecting those associated with other vertices [44]. The PV is required to be within 15 cm of the CMS detector center in the z direction to ensure optimal reconstruction efficiency.

Jets are reconstructed from the PF particles using the anti- k_T algorithm [45, 46] with a distance parameter of 0.4. The jet momentum (energy) is calculated as the vectorial (scalar) sum of the momenta (energies) of all clustered particles. Corrections derived from data and simulation are applied to the jet energy. Jets that are consistent with the fragmentation of b quarks (b jets) are identified using the DEEPJET discriminator [47–49]. Both the medium and loose working points are used; the medium (loose) working point has an 85% (90%) probability of correctly identifying b jets with $p_T > 90$ GeV and a 1% (10%) probability of misidentifying light-flavor jets as b jets. The scalar p_T sum of all jets within an event (H_T) is used to select energetic events.

The analysis considers data collected using triggers based on jet p_T and on H_T calculated from the summed p_T of online-reconstructed jets. The trigger used for the data collected in 2016 requires at least one jet with $p_T > 450$ GeV or $H_T > 900$ GeV, while for 2017–2018, the H_T threshold is increased to 1050 GeV and there is no p_T requirement. The inclusion of a jet

$m_{X_{\text{dark}}}$ [GeV]	$m_{\pi_{\text{dark}}}$ [GeV]	κ_0 value				
1000	6	0.92	0.61	0.53	0.43	0.29
	10	0.62	0.42	0.36	0.30	0.20
	20	0.37	0.25	0.21	0.18	0.12
1200	6	1.10	0.73	0.63	0.52	0.35
	10	0.75	0.50	0.43	0.35	0.24
	20	0.45	0.30	0.26	0.21	0.14
1400	6	1.28	0.86	0.74	0.61	0.41
	10	0.87	0.58	0.50	0.41	0.28
	20	0.52	0.35	0.30	0.25	0.16
1600	6	1.47	0.98	0.85	0.69	0.46
	10	1.00	0.67	0.58	0.47	0.32
	20	0.59	0.40	0.34	0.28	0.19
1800	6	1.65	1.10	0.95	0.78	0.52
	10	1.12	0.75	0.65	0.53	0.36
	20	0.67	0.45	0.39	0.32	0.21
2000	6	1.83	1.23	1.06	0.87	0.58
	10	1.25	0.84	0.72	0.59	0.40
	20	0.74	0.50	0.43	0.35	0.23
2200	6	2.02	1.35	1.16	0.95	0.64
	10	1.37	0.92	0.79	0.65	0.43
	20	0.82	0.55	0.47	0.39	0.26
2400	6	2.20	1.47	1.27	1.04	0.70
	10	1.50	1.00	0.87	0.71	0.47
	20	0.89	0.60	0.51	0.42	0.28
2500	6	2.29	1.53	1.32	1.08	0.72
	10	1.56	1.04	0.90	0.74	0.49
	20	0.93	0.62	0.54	0.44	0.29

Table 2. Parameters used for the flavor-aligned model. In order to probe a range of lifetimes, the values of κ_0 listed in columns 3–7 are tuned to give the desired $c\tau_{\pi_{\text{dark}}}^{\text{max}}$ values of 5, 25, 45, 100, and 500 mm. In addition, samples were made with fixed $\kappa_0 = 1$, with a resultant value of $c\tau_{\pi_{\text{dark}}}^{\text{max}}$ that depends on the other model parameters.

p_T trigger requirement for 2016 was necessary because, in part of the 2016 data taking period, some jets reaching the saturation energy for the level-1 trigger were mistakenly dropped from the H_T sum, resulting in a significant loss of efficiency. This loss was recovered by including the single-jet trigger requirement. The H_T threshold was increased in 2017 to compensate for the higher instantaneous luminosity. The efficiencies for an event to pass any of these trigger conditions in both data and simulation are measured from data sets collected with an independent trigger that requires a muon with $p_T > 50 \text{ GeV}$. In both cases, the efficiencies are close to unity above the signal selection H_T thresholds, and the difference between the efficiencies as measured in simulation and data is applied as a correction to the simulation.

5 Analysis

The offline analysis selects energetic events with at least four jets. Jets are classified as EJ candidates using information from tracks associated with the jets. An overview of the event selection strategy is given in section 5.1. Descriptions of the “candidate” EJ identification criteria (“tagging”) is given in section 5.2. The algorithms used to optimize the selection criteria to maximize signal sensitivity, and the resulting event selection requirements are described in section 5.3.

5.1 Event and physics object selection

While some SM hadrons, such as those containing b quarks, have macroscopic decay lengths, tracks associated with SM jets mainly come from particles produced promptly (close to the collision primary vertex). In EJs, when the lifetime of one or more of the dark mesons is long, a substantial fraction of the tracks can emerge from displaced vertices. In addition, in the flavor-aligned scenario, most of the dark pion decay products are b quarks, which results in displaced tracks even when the dark pion decays immediately. We use as our displacement measure the d_{xy} (d_z), measured from the PV to the point of closest approach on the track trajectory, as this gives better sensitivity than reconstructing individual decay vertices. Jets used in this analysis are required to have $p_T > 100 \text{ GeV}$, as we are looking for EJs originating from a heavy-mediator decay, and $|\eta| < 2$, to ensure that they are well contained in the tracker. Jet candidates are also required to pass a set of quality criteria to reject spurious jets from instrumental sources [50]. To reduce the probability of displaced tracks being incorrectly assigned to jets by the PF algorithm, high-purity tracks, as defined in ref. [23], with $p_T > 1 \text{ GeV}$ are associated with jets by requiring the angular separation between the jet direction and the track direction, $\Delta R = \sqrt{(\Delta\eta)^2 + (\Delta\phi)^2} < R_{\max}$, where $\Delta\eta$ is the η separation between the jet axis and the track, and $\Delta\phi$ is the separation in the azimuthal direction. We also reject tracks with $|d_z| > d_z^{\max}$ to suppress jets from pileup interactions. The values of R_{\max} and d_z^{\max} are optimized for each signal model. If a track can be assigned to multiple jets, it is assigned to the jet with the smallest ΔR separation. Jets are required to have at least one associated track so that the jet displacement measure can be calculated. To suppress events with a poorly reconstructed PV, we require that at least 10% of associated tracks have a longitudinal displacement from the PV less than 0.01 cm.

Candidate signal events are required to have high H_T and at least four jets passing the criteria above. At least two of these four jets must be tagged as EJs. If more than

four jets are found, the four jets with the largest p_T are used. The H_T and EJ criteria are optimized for each signal model.

5.2 EJ tagging

Two EJ tagging strategies are used in this analysis. The first selects candidate EJs via requirements on jet-level variables using track displacement measures (“model-agnostic selection”). The second uses a graph neural network trained on specific signal models to determine an EJ tagging score (“machine learning or ML-based selection”). The model-agnostic method allows for a simpler reinterpretation of the results for alternate theoretical models not considered in this paper, while the ML-based approach achieves the best possible sensitivity for the specific models studied here.

The model-agnostic EJ tagger uses different input features for the unflavored and flavor-aligned dark sector models, while the ML-based EJ tagger is trained separately for each class of model.

5.2.1 Model-agnostic EJ tagging

For the EJ tagging that targets the unflavored dark sector models, $R_{\max} = 0.4$ is used. The following variables, which were also used in ref. [21], are used for the EJ tagging:

- $\langle d_{xy} \rangle$: this is the median d_{xy} of tracks associated with a jet.
- α_{3D} : this is defined as

$$\alpha_{3D} = \frac{\sum_{D_N < D_N^{\max}} p_T^{\text{track}}}{\sum p_T^{\text{track}}},$$

which is the ratio between the scalar p_T sum of the associated tracks with a pseudo-significance D_N smaller than the selection value D_N^{\max} and the scalar p_T sum of all the associated tracks. The pseudo-significance D_N is defined as:

$$D_N = \sqrt{\left(\frac{d_z}{0.01 \text{ cm}}\right)^2 + \left(\frac{d_{xy}}{\sigma(d_{xy})}\right)^2},$$

where $\sigma(d_{xy})$ is the d_{xy} uncertainty calculated from the covariance matrix of the fitted track trajectory. The d_z significance is based on the PV z resolution.

The distributions of these variables are presented in figure 2 for data events and for simulated signal and multijet background events. The data and simulated events shown require $H_T > 1200 \text{ GeV}$ and at least four jets with $p_T > 100 \text{ GeV}$ and $|\eta| < 2$, which is much less restrictive than the final signal selection requirements.

The flavor-aligned dark sector model has three different dark meson lifetime ranges: long-lived dark mesons (up to 50 cm for the κ_0 parameters considered in this search), dark mesons with a b-hadron-like displacement from prompt dark meson decays into b quarks, and dark mesons that decay promptly into light SM quarks. In addition, since at least one dark quark in the flavor-aligned model couples to the b quark, the jets often contain heavy-flavor hadrons, and the resulting EJ is wider than that of the unflavored model. Because of this, the tagging of EJs in the flavor-aligned model associates tracks with a jet using a proximity measure of $R_{\max} = 0.8$. The selection for candidate flavor-aligned EJs is based on the following variables:

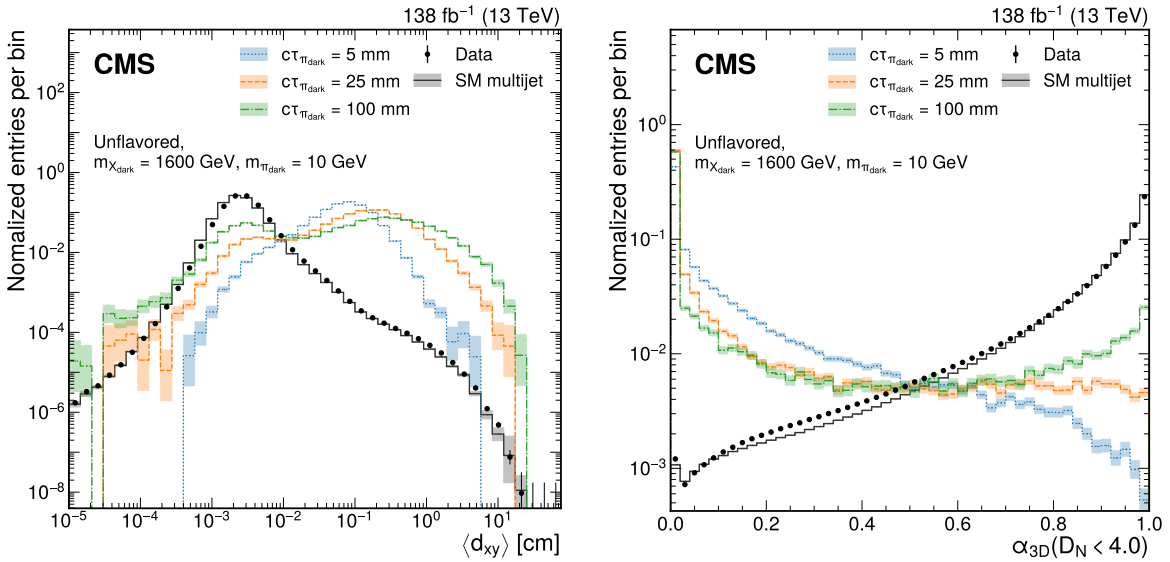


Figure 2. Distributions of the jet variables $\langle d_{xy} \rangle$ (left) and α_{3D} with $D_N^{\max} = 4$ (right) used for the model-agnostic EJ tagging that targets the unflavored dark sector models are shown for data (points), SM multijet simulation (gray line), and signal jets in simulation (colored lines). The sums of the entries are normalized to unity.

- $n_{\text{track}}^{d_{xy} > d_{xy}^{\min}}$, the number of tracks with d_{xy} greater than a threshold d_{xy}^{\min} : this quantity exploits the tendency of the flavor-aligned dark sector to generate multiple long-lived SM mesons in the particle shower, resulting in a large number of displaced tracks.
- Jet girth: this is defined as the p_T -weighted ΔR separation of tracks from the jet direction:

$$\text{Jet girth} = \frac{\sum_i p_T^i \Delta R(i, \text{jet})}{\sum_i p_T^i},$$

where the index i runs over all tracks associated with the jet of interest. This variable exploits the feature that particles in EJs tend to have a wider angular separation than SM jets because of the large mass of the dark mesons.

Figure 3 shows the distributions of the tagging variables used in the flavor-aligned analysis for data, simulated signal, and multijet background events. The data and simulated events follow the same requirements as those appearing in figure 2.

As the jet-track association radius $R_{\max} = 0.8$ is larger than the $R = 0.4$ value used to perform jet clustering, jets that have nearby soft jets can be misidentified as EJs. To remove these candidates, a modified N -subjettiness variable $\bar{\tau}_n$ is calculated as follows:

1. For each of the four candidate high- p_T jets, we consider all jets within $\Delta R < 0.8$ of the selected jets that have $p_T > 30 \text{ GeV}$ in decreasing order of jet p_T . These will be used as the “subjet” collection to calculate $\bar{\tau}_n$. Using this definition, all candidate jets will have at least one subjet: the candidate jet itself.

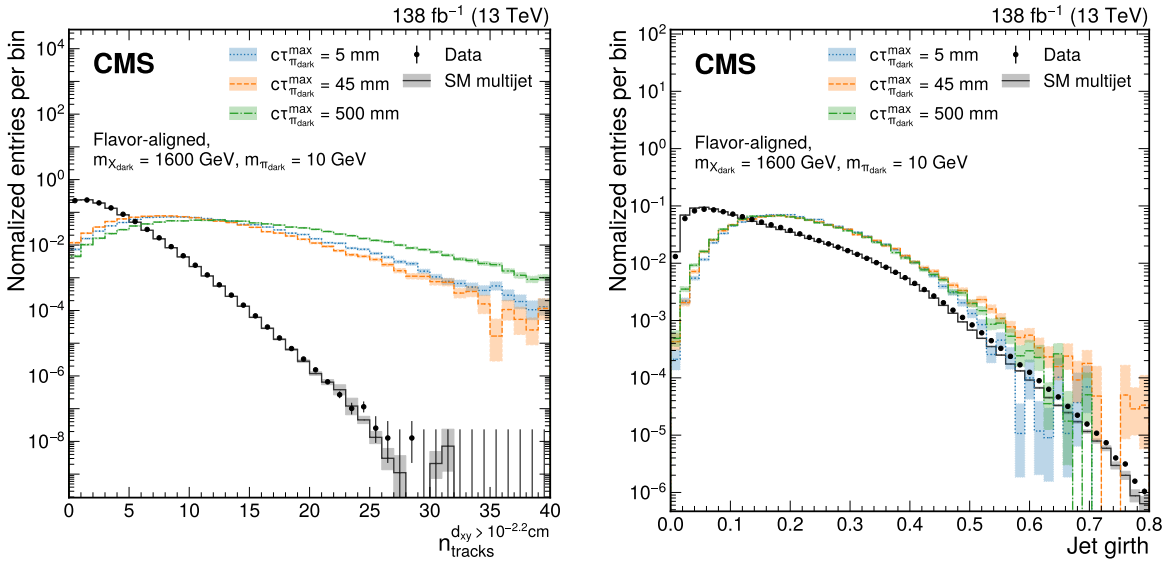


Figure 3. Distributions of the jet variables used for the model-agnostic EJ tagging targeting flavor-aligned dark sector models for jets obtained in data (points), SM multijet simulation (gray line), and simulated signal jets (colored lines). The distribution of the number of tracks with $d_{xy} > 10^{-2.2}$ cm (jet girth) is shown on the left (right). The sums of the entries are normalized to unity.

- After determining the subjet collection assigned to each candidate jet, the computation of $\bar{\tau}_n$ is then carried out up to the leading n subjets:

$$\bar{\tau}_n = \frac{\sum_i p_T^i \min\{\Delta R_{ij}\}}{\sum_i 0.8 p_T^i},$$

similar to the definition of the original N -subjettiness [51]. The index i runs over the tracks associated with the candidate jet, and j runs from 1 up to n for the subjet collection assigned to the selected jet.

The requirement that $\bar{\tau}_{2/1} = \bar{\tau}_2 / \bar{\tau}_1 > 0.5$ is applied to all EJ candidates and is found to reliably suppress the misidentification of SM jets with nearby soft jets as EJs.

5.2.2 The ML-based EJ tagging

The ML-based tagger uses a graph neural network (GNN) based on PARTICLENET [52] to directly incorporate the track information. Two separate GNNs are trained to classify EJs: one for the unflavored model (uGNN) and the other for the flavor-aligned model (aGNN). Each is trained, validated, and tested using all of the EJs from the signal samples and an equal number of background jets from background samples, weighted equally. The training, validation, and testing data subsets make up 60%, 15%, and 25% of the full data set, respectively. The output of each GNN is a score ranging from 0 to 1, which is a measure of the probability that the jet is an EJ. Tracks are associated with a jet using $R_{\text{max}} = 0.8$. To maximize the available information for the ML training, the tracks are not required to satisfy a d_z^{max} requirement. Each network is trained on all jets originating from a dark quark in the signal models of interest, and an equal number of jets taken from SM QCD simulation as the background sample.

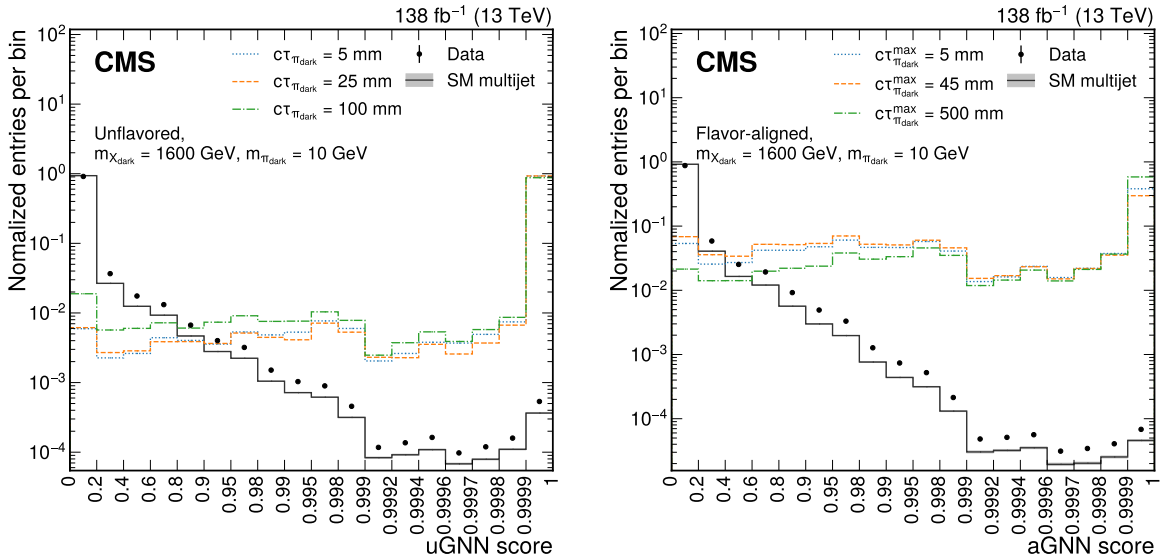


Figure 4. Distributions of the output score of the uGNN (left) and aGNN (right) for the data (points with error bars), SM multijet simulation (dark gray line), and signal simulation (colored lines). The signal distributions in the left (right) plot are generated from the unflavored (flavor-aligned) model. Bins are chosen to correspond to the jet selection criteria defined in table 5. The uncertainties in the SM multijet simulation are too small to be visible. The systematic uncertainties in the simulated signal distributions are small and have been omitted for reasons of clarity. The sums of the entries are normalized to unity.

The $\Delta\eta$ and $\Delta\phi$ between each track and its associated jet are used as the track coordinate variables in the jet space. Each track in the jet is represented by a 5-feature vector containing:

- $\Delta R(\text{track}, \text{jet})$, as particles in EJs tend to have a wider angular separation than in the SM jets because of the heaviness of the dark mesons.
- $\ln(p_T^{\text{track}}/1\text{ GeV})$, $\ln(p_T^{\text{track}}/\sum_i p_T^i)$, as the combination of the dark shower and the decay of the mesons back to the SM sector causes the p_T of tracks to be smaller on average for EJs than for SM jets.
- $T(d_{xy})$, $T(d_z)$. The transformation function $T(x)$ is applied to the track displacement variables, to reduce the range of values input to the GNN while preserving the variables' sign and continuity. It is defined as:

$$T(x) = \text{sign}(x) \ln \left(\left| \frac{x}{1\text{ cm}} \right| + 1 \right).$$

This transformation was found to give comparable or better performance than a standard scaling.

The impact parameter d_{xy} is the most influential feature. Figure 4 shows the output score distributions for signal and background, demonstrating good separation. The signal distributions are similar despite the wide range of dark meson $c\tau$ values.

5.3 Determining the EJ tagging and event selection criteria

Searches for each of the signal models listed in tables 1 and 2 are conducted. An optimization procedure is performed for each signal model to determine the best threshold on the event H_T , jet p_T , and the EJ tagging variables by maximizing σ_{opt} , defined as:

$$\sigma_{\text{opt}} = \frac{S}{\sqrt{S + B + \beta^2 B^2}}, \quad (5.1)$$

where S (B) is the number of simulated signal (background multijet) events passing the selection thresholds and β is the estimated relative systematic uncertainty in the background, taken to be 10%. To reduce the number of sets of selection criteria, similar selection sets are grouped, and a representative set that gives at least 90% of the original best significance value is used for all the models in the group. Additional selection sets with higher background selection efficiencies are used to validate the background estimation calculations. Their selection criteria are detailed in section 6.

The selection criteria used for EJ tagging are shown in tables 3–5, and those for the event selection in table 6. In the model-agnostic approach, longer signal model lifetimes in the unflavored scenario tend to favor selection criteria with larger $\langle d_{xy} \rangle$ selection thresholds. On the other hand, in the flavor-aligned scenario, longer signal model lifetimes favor selection criteria with higher d_{xy}^{\min} thresholds. In the ML-based approach, GNN EJ taggers generally exhibit consistent performance across varying signal model lifetimes, and the signal models with larger mediator particle masses generally are targeted by selection criteria with higher H_T threshold. The specific selection criteria employed for each EJ model, along with the signal selection efficiency for each model under various selection criteria, are documented in the HEPdata record [22]. For the unflavored model, at $c\tau_{\pi_{\text{dark}}} = 45$ mm, the model-agnostic taggers yield a maximum signal selection efficiency of $\approx 40\%$, while the ML-based taggers yield a maximum signal selection efficiency of $\approx 60\%$. The signal selection efficiency of the model-agnostic taggers drops to a few percent for very short-lived (≈ 1 mm) dark pions, and the efficiency of both taggers drops to a few percent for very long-lived (≈ 1000 mm) dark pions. For the flavor-aligned model, at $c\tau_{\pi_{\text{dark}}}^{\max} = 45$ mm, the model-agnostic taggers yield a maximum signal selection efficiency of $\approx 25\%$, while the ML-based taggers yield a maximum signal selection efficiency of $\approx 40\%$. This efficiency remains fairly stable along the full maximum proper lifetime range for both taggers.

6 Background estimation

The signal region (SR) for this analysis is constructed from events with two or more tagged EJs. The main source of background for this analysis is the production of four SM jets, where two or more of these jets are misidentified as EJs. We estimate the number of SM events passing each selection criteria in the SR by constructing a control region (CR) with identical event and jet kinematic requirements, but where exactly one jet is tagged as an EJ. We estimate the fraction of signal events in the CR to be no more than 10^{-5} . The probability of an SM jet being misidentified as an EJ (mistag rate) is heavily dependent on the underlying jet flavor, as SM jets containing b hadrons also have displaced tracks. We therefore estimate

Tag name	d_z [cm] (<)	$\langle d_{xy} \rangle$ [cm] (>)	D_N (<)	α_{3D} (<)
u-tag 1	0.5	$10^{-1.6}$	4.0	0.25
u-tag 2	1.0	$10^{-1.4}$	8.0	0.25
u-tag 3	5.0	$10^{-1.2}$	8.0	0.25
u-tag 4	5.0	$10^{-1.2}$	12.0	0.15
u-tag 5	5.0	$10^{-1.0}$	12.0	0.15
validation u-tag	0.5	$10^{-1.6}$	4.0	0.40

Table 3. Emerging jet selection criteria for the model-agnostic analysis designed for the unflavored scenario. The validation regions are discussed in section 6. The symbols in parentheses indicate a minimum (>) or maximum (<) requirement.

Tag name	d_z [cm] (<)	d_{xy}^{\min} [cm]	$n_{\text{track}}^{d_{xy} > d_{xy}^{\min}}$ (>)	Jet girth (>)
a-tag 1	0.5	$10^{-2.2}$	12	0.05
a-tag 2	0.5	$10^{-2.2}$	12	0.1
a-tag 3	0.5	$10^{-2.3}$	14	0.0
a-tag 4	0.5	$10^{-2.4}$	14	0.1
validation a-tag	0.5	$10^{-2.4}$	12	0.0

Table 4. Emerging jet selection criteria for the model-agnostic analysis designed for the flavor-aligned scenario. The validation tag is described in section 6. The symbols in parentheses indicate a minimum (>) or maximum (<) requirement.

Tag name	Score min.	Score max.
uGNN tag 1	0.9997	1
uGNN tag 2	0.9998	1
uGNN tag 3	0.9996	1
uGNN validation tag	0.998	0.9995
<hr/>		
aGNN tag 1	0.9953	1
aGNN tag 2	0.9993	1
aGNN tag 3	0.9983	1
aGNN validation tag	0.99	0.995

Table 5. The GNN score range used to identify a jet as an EJ. The uGNN (aGNN) tag indicates that the tagger uses the output score of the GNN trained on the unflavored (flavor-aligned) simulated signal samples. The validation tags are described in section 6.

Selection set	H_T [GeV]	Jet p_T [GeV] (>)					EJ tagger
u-set 1	>1600	275	250	250	150		u-tag 1
u-set 2	>1600	200	200	150	150		u-tag 2
u-set 3	>1600	200	150	100	100		u-tag 3
u-set 4	>1500	200	150	100	100		u-tag 4
u-set 5	>1200	200	150	100	100		u-tag 5
u-set validation	1000–1200	100	100	100	100		validation u-tag
a-set 1	>1500	200	150	100	100		a-tag 1
a-set 2	>1800	250	250	200	200		a-tag 2
a-set 3	>1200	275	250	250	200		a-tag 2
a-set 4	>1500	275	250	250	100		a-tag 3
a-set 5	>1800	200	150	100	100		a-tag 4
a-set validation	1000–1200	100	100	100	100		validation a-tag
uGNN set 1	>1350	170	120	120	100		uGNN tag 1
uGNN set 2	>1750	300	260	250	250		uGNN tag 2
uGNN set 3	>1800	240	180	180	100		uGNN tag 3
uGNN validation	>1000	100	100	100	100		uGNN validation tag
aGNN set 1	>1300	200	140	120	100		aGNN tag 1
aGNN set 2	>1650	300	250	200	200		aGNN tag 2
aGNN set 3	>1400	270	220	220	120		aGNN tag 3
aGNN validation	>1000	100	100	100	100		aGNN validation tag

Table 6. Event selection criteria used for the analysis. The validation selection criteria are described in section 6.

the misidentification probability $\epsilon(f, p_T)$ as a function of the underlying jet flavor f , where f is b for b jets and q for other jet flavors, and the jet p_T .

When the probability of a jet being misidentified as an EJ is characterized and parameterized using p_T , flavor fraction, and jet type, the number of background events in the SR is estimated using counts in the CR and the mistag rate according to the following formula:

$$N_{\text{SR}} = \sum_{\text{events} \in \text{CR}} \frac{\frac{1}{2!} \left(\sum_i \epsilon_i \prod_{j \neq i} (1 - \epsilon_j) \right) + \frac{1}{3!} \left(\sum_{i \neq j} \epsilon_i \epsilon_j \prod_{k \neq i,j} (1 - \epsilon_k) \right) + \frac{1}{4!} \left(\sum_{i \neq j \neq k} \epsilon_i \epsilon_j \epsilon_k \right)}{\prod_i (1 - \epsilon_i)}, \quad (6.1)$$

where ϵ_i is an abbreviation of $\epsilon(f_i, p_T^i)$, the estimated mistag rate of jet i in each event. The jet indices in the summations and products run over all jets that are not EJ tagged. The denominator calculates the fraction of events that have exactly one EJ-tagged jet, while the three terms in the numerator calculate the fractions of events with two, three, and four EJ-tagged jets, respectively. The common factor for the estimated mistag rate for the

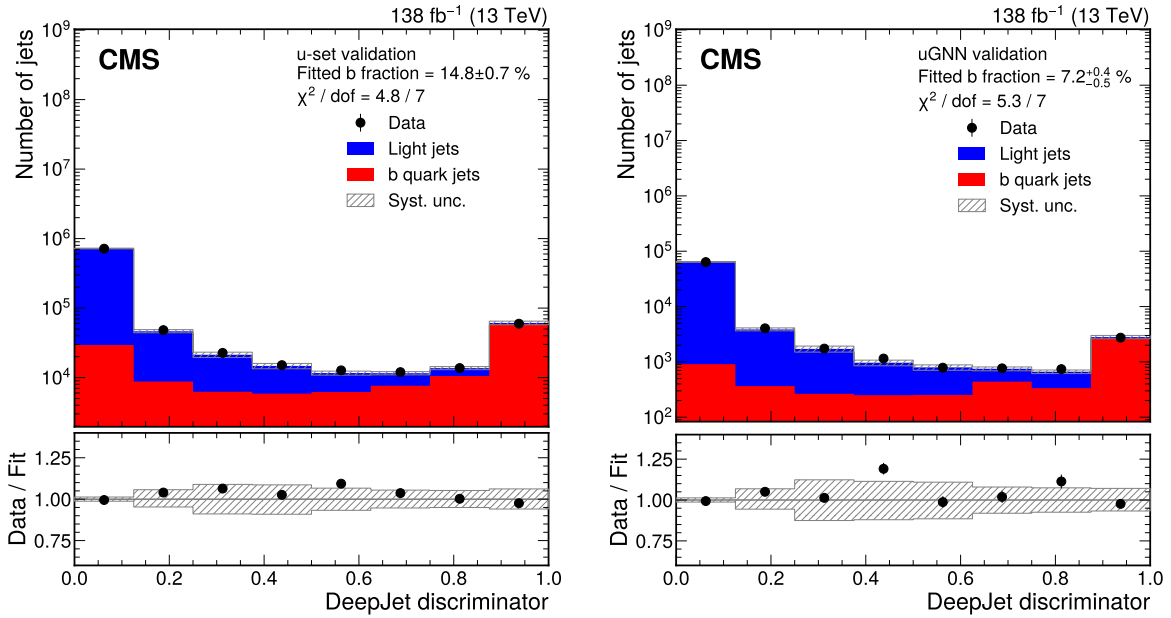


Figure 5. Template fit of the DEEPJET discriminator used to determine the b jet fraction of the non-EJ tagged jets for data events that pass the “u-set validation” (uGNN validation) selection criteria shown on the left (right), except with the requirement on the number of EJ-tagged jets changed from 2 to 1. The lower panels show the ratio of the number of jets in the data compared to the sum of the fitted template distributions.

EJ-tagged jet exists in both the numerator and denominator, and therefore does not appear in the expression. The factorials in the numerator are needed to correct for repeated counting in the unordered sum over the jet indices. For example, the first term in the numerator needs a factor 2! to correctly handle events where the two highest p_T jets are tagged as EJs and the next two jets are not tagged; without this factor, the unordered sum would count these events twice. A detailed derivation of the equation is given in ref. [53]. Because the underlying flavor of each jet is difficult to determine, we approximate ϵ_i in eq. (6.1) using a flavor-fraction-averaged misidentification rate $\epsilon^{\text{avg}}(p_T)$ and the estimated b jet fraction F_b^{CR} of all non-EJ-tagged jets in the CR:

$$\epsilon^{\text{avg}}(p_T) = F_b^{\text{CR}} \epsilon(b, p_T) + (1 - F_b^{\text{CR}}) \epsilon(q, p_T). \quad (6.2)$$

The value of F_b^{CR} is estimated by fitting the CMS DEEPJET discriminator [47] spectrum of the non-EJ-tagged jets in the CR to two template distributions obtained from SM multijet MC events. One template contains the discriminator value for jets identified using generator-level information as containing a b quark, and the complement template is used for the other jets. The template distributions are varied within the measured uncertainties [48, 49]. The normalization factor of the b quark template, F_b^{CR} , is the only free parameter. The fit is performed for each of the selection criteria listed in table 6. Figure 5 gives an example of the fit performance for the “u-set validation” and the “uGNN validation” selection criteria, defined in table 6.

The evaluation of the mistag rate is performed in a signal-free region (FR) that consists of events passing a high- p_T photon trigger and containing an isolated photon in the ECAL barrel with $p_T > 200$ GeV. The FR events are required to have either one or two jets passing the jet selection criteria described in section 5.1. To obtain the misidentification probability for different jet flavors, we further divide the FR into a b-enriched region (ER) and a b-depleted region (DR) by imposing b tagging requirements on an additional jet with $p_T > 50$ GeV and $|\eta| < 2.4$ that passes a set of noise-rejection criteria [50]. As a significant fraction of heavy-flavored jets originate from gluon splitting in this event sample, b tagging requirements on this extra jet will change the b jet fraction of the selected jets. Events are classified as ER if the additional jet passes DEEPJET b tagging at the medium working point, and are classified as DR if the additional jet fails DEEPJET b tagging at the loose working point. Assuming that the ER and DR have the same mistag probabilities for the selected jets, and the only difference between these regions is the overall b jet fraction, the misidentification rate for all the selected jets in a specific region XR, $\epsilon^{\text{XR}}(p_T)$, can be expressed as a linear combination of $\epsilon(b, p_T)$ and $\epsilon(q, p_T)$:

$$\begin{aligned}\epsilon^{\text{ER}}(p_T) &= F_b^{\text{ER}}(p_T)\epsilon(b, p_T) + \left(1 - F_b^{\text{ER}}(p_T)\right)\epsilon(q, p_T), \\ \epsilon^{\text{DR}}(p_T) &= F_b^{\text{DR}}(p_T)\epsilon(b, p_T) + \left(1 - F_b^{\text{DR}}(p_T)\right)\epsilon(q, p_T),\end{aligned}\quad (6.3)$$

where $F_b^{\text{XR}}(p_T)$ is the estimated b jet fraction of region XR in bins of jet p_T . The b jet fraction is obtained by fitting the DEEPJET b discriminator distribution to templates obtained using jets from a simulated γ +jets sample. On average, the selected jets in the ER and DR have b jet fractions of 15% and 4%, respectively. The linear relation in eq. (6.3) can then be inverted to obtain the mistag rates for different underlying jet flavors $\epsilon(f, p_T)$, which is used in eq. (6.2) to estimate the misidentification rate of jets in the CR. Figure 6 gives examples of the estimated EJ tagger misidentification probabilities for “u-tag 1” and “uGNN tag 1” taggers, defined in tables 3 and 5.

Because the Phase 1 upgrade of the pixel detector [24] improved the track reconstruction performance, the evaluation of the expected background is performed separately for the pixel Phase 0 geometry (2016) and Phase 1 geometry (2017–2018).

6.1 Validation tests

To validate the background estimation by checking the soundness of the calculations, closure tests are performed in validation regions (VRs) that use selection criteria that are orthogonal to the SRs. The VRs are defined using signal-like selection criteria that require at least two jets passing a validation EJ tagger. The observed number of events in the VR is compared to the number predicted using our background estimation technique. For the model-agnostic EJ tagging VR, the H_T requirement of the validation event selection is inverted to ensure orthogonality with the SRs and small signal contamination. The EJ identification requirements for the validation EJ tagger are based on the u-tag 1 and a-tag 1 requirements for unflavored and flavor-aligned models, respectively, with one jet-variable selection requirement relaxed to further reduce the effect of any small signal contamination. The VR for the ML-based EJ tagging uses a validation tagger that selects jets with GNN

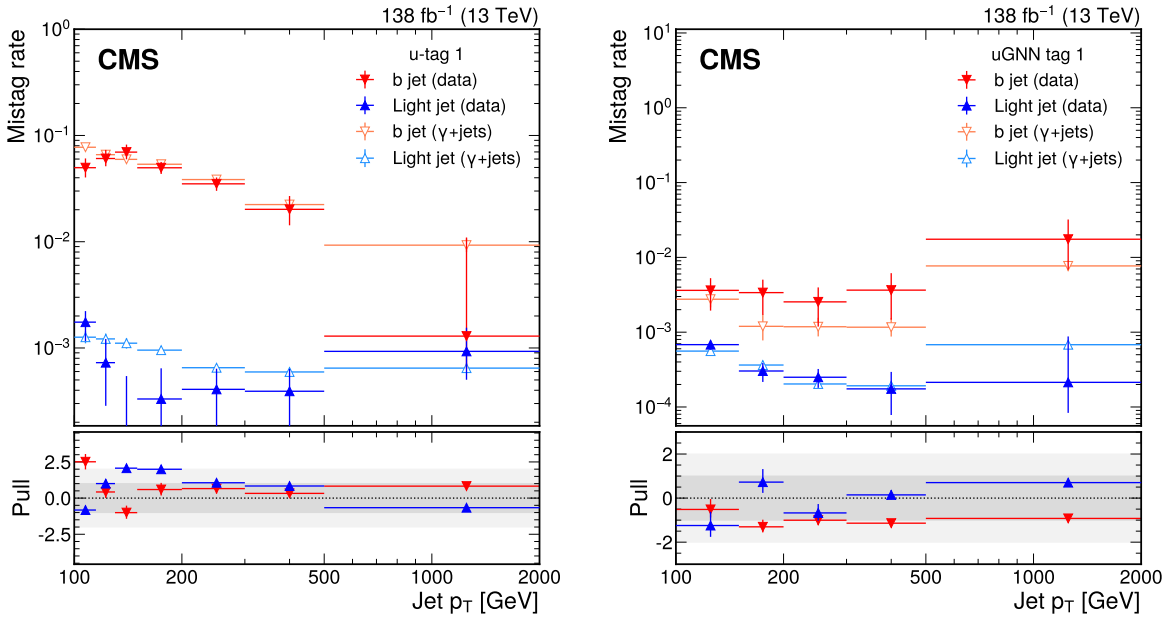


Figure 6. The EJ tagger misidentification probability for b quark jets (red, orange) and light jets (light blue, dark blue) as a function of jet p_T for the model-agnostic tagger “u-tag 1” (left) and the ML-based tagger “uGNN tag 1” (right), as defined in tables 3 and 5, evaluated using data (red, dark blue) and generator-level flavor information from simulated samples (orange, light blue) in events containing a high- p_T photon. The lower panel shows the pull, defined as the difference between the mistag rate calculated in simulation and mistag rate measured in data, scaled down by the uncertainty measured in data. The error bars indicate the uncertainties in the mistag rates measured in simulation scaled by the uncertainties measured in data.

scores in a region disjoint from the SRs. To further increase the number of events that pass the ML-based VR, we relax the H_T and jet p_T requirements. The full list of the selection criteria used for the VRs is given in tables 3–6. The signal contamination in these VRs is less than 1% for all surveyed signal models.

The number of events passing the VR selection criteria with at least two jets passing the validation jet tag, as well as the predicted number using the estimation described in eq. (6.1), is given in table 7. No significant deviation between the observed and the estimation results is observed, indicating that the background estimation calculation is robust.

7 Systematic uncertainties

7.1 Background uncertainties

The main sources of systematic uncertainty in this search arise from the background estimation method based on control samples in data. The kinematic differences between the SM jets in the CR photon-triggered data used for the misidentification rate calculation and the SM jets in the H_T -triggered data used in the SR may lead to slightly different misidentification rates. We estimate the corresponding uncertainties by applying the background prediction method in eq. (6.1) to simulated SM multijets events, using either the mistag rate from the SM multijet simulation or from the γ +jets simulation. The uncertainty is taken as the difference in the

Selection set	Estimation \pm stat. \pm syst.			Observed yield
u-set validation	1220	$^{+ 80}_{- 80}$	± 210	1484
a-set validation	77	$^{+ 4}_{- 4}$	± 15	118
uGNN validation	29.3	$^{+ 7.0}_{- 3.4}$	± 8.2	21
aGNN validation	29.1	$^{+ 6.1}_{- 2.6}$	± 5.2	37

Table 7. The observed yield of events in data satisfying the validation selection criteria with at least two jets passing the corresponding validation tag, and the estimation based on the misidentification rate calculated using validation events with exactly one jet passing the validation tagger scaled by the factor given in eq. (6.1). The statistical and systematic uncertainties are reported for the estimated yields.

Uncertainty source	Model-agnostic taggers				ML-based taggers			
	Unflavored		Flavor-aligned		Unflavored		Flavor-aligned	
	mean	std.	mean	std.	mean	std.	mean	std.
Parameterization	27.0	7.3	11.8	0.9	8.3	3.3	44.6	9.9
CR/VR differences	6.4	2.4	11.1	5.4	16.4	9.1	12.3	2.9
Jet flavor evaluation	10.7	2.2	24.5	6.3	10.5	1.8	15.5	6.5

Table 8. Mean and standard deviation (std.) of the relative uncertainty calculated on the background estimations, by source, in percent.

background predictions obtained with the two mistag rates. There is also an uncertainty in the flavor composition used in the misidentification rate estimations. This uncertainty is estimated from simulated background events by comparing the flavor-decomposition estimate described in section 6 with one derived from generator-level flavor information. Finally, there is the uncertainty associated with the choice of variables used to parameterize the mistag rate. This uncertainty is estimated by comparing the estimation results when parameterizing the mistag rate as a function of jet p_T versus track multiplicity, and as a function of coarse versus fine p_T binning, as the mistag rate has a significant dependence on the parameter chosen and binning scheme used. The uncertainties in the flavor composition and mistag rate parameterization are larger on average than the uncertainty due to CR and SR differences. The model-agnostic method is more affected by changes in the chosen mistag rate parameter because the jet-level variables used depend on track multiplicity. The GNN method is more sensitive to the mistag rate binning scheme because of statistical fluctuations due to the small number of jets in some of the bins. The contribution of all the background uncertainty sources for various signal model search regions is summarized in table 8. These three uncertainty sources are considered to be uncorrelated and summed in quadrature. The resulting uncertainties are given in tables 7 and 10. The difference between the observed and estimated yields in the a-set validation, shown in table 7, was investigated. No anomaly was found in the data, and thus it is assumed to arise from a statistical fluctuation.

Uncertainty source	Model-agnostic taggers				ML-based taggers			
	Unflavored		Flavor-aligned		Unflavored		Flavor-aligned	
	mean	std.	mean	std.	mean	std.	mean	std.
Integrated luminosity	1.8	0.6	1.8	0.6	1.8	0.6	1.8	0.6
Trigger efficiency	0.3	0.1	0.3	0.1	0.3	0.1	0.3	0.1
JES	1.0	1.3	0.8	0.7	1.3	0.9	0.7	0.4
JER	0.3	0.4	0.3	0.3	0.2	0.3	0.2	0.1
Pileup reweighting	1.6	1.4	1.4	1.2	0.9	0.8	1.0	0.9
Track modeling in sim.	0.2	0.3	1.4	1.8	0.3	0.8	0.5	0.6
PDF	<0.1	<0.1	<0.1	<0.1	<0.1	<0.1	<0.1	<0.1
μ_F, μ_R	<0.1	<0.1	<0.1	<0.1	<0.1	<0.1	<0.1	<0.1

Table 9. Mean and standard deviation (std.) of the relative uncertainty calculated on the unflavored and flavor-aligned samples, by source, in percent.

7.2 Signal uncertainties

Various sources of uncertainty affecting the signal yields are also considered. The integrated luminosity uncertainties for the 2016, 2017, and 2018 data-taking periods are 1.2, 2.3, and 2.5%, respectively [54–56]. There is a small difference in the trigger efficiency between data and simulation, with a ratio varying between 0.95 and 1.00. A correction factor compensates for this difference, and its statistical uncertainty is propagated to an uncertainty in the signal acceptance. The evaluation of jet energy correction uncertainties is performed as a function of jet p_T and η , propagated to all jet-related kinematic variables, and then to an uncertainty in the signal acceptance. Uncertainty sources are treated as fully correlated across the years for the jet energy scale (JES), and uncorrelated for the jet energy resolution (JER). While the pileup distribution in the simulation is reweighted to match the data, there is a 4.6% uncertainty in the total inelastic cross section [57], which is treated as fully correlated across the years. The impact parameter distribution is slightly broader in the data CRs than in simulation. A smearing function that corrects this is applied to tracks in the simulated samples, and the resulting changes to the signal acceptances are used to estimate the modeling uncertainty. The corrected values are also used to recompute the GNN score. The uncertainty in the acceptance from the uncertainties in the PDFs is evaluated by reweighting events with different PDF variations [35, 58]. As reconstruction efficiency differences between data and simulation for displaced tracks are difficult to evaluate, we varied the reconstruction efficiency for tracks with $d_{xy} > 4$ cm (approximately the distance to the second layer of the pixel detector) by 10% and found an $\approx 1\%$ overall change in signal acceptance. As the measured difference in reconstruction efficiency in data and MC is expected to be much smaller [59, 60], no uncertainty is assigned. The uncertainty from the factorization scale (μ_F) and renormalization scale (μ_R) choices is estimated by independently varying μ_F and μ_R by factors of 2 and 0.5 [61, 62]. A summary of the estimated uncertainties for the various signal model acceptances is given in table 9.

Selection set	Estimation	\pm stat.	\pm syst.	Observed yield
u-set 1	56	± 9	± 20	67
u-set 2	20.0	± 4.3	± 7.0	21
u-set 3	22.9	± 7.3	± 4.9	24
u-set 4	7.9	± 2.0	± 2.2	10
u-set 5	11.3	± 2.7	± 2.0	13
a-set 1	8.8	± 2.4	± 2.0	16
a-set 2	1.67	± 0.49	± 0.38	3
a-set 3	1.97	± 0.47	± 0.37	2
a-set 4	2.30	± 0.81	± 0.39	3
a-set 5	10.2	± 2.3	± 3.4	16
uGNN set 1	15.6	± 5.4	± 3.8	18
uGNN set 2	0.73	± 0.44	± 0.27	0
uGNN set 3	7.6	± 3.5	± 2.3	9
aGNN set 1	45	± 18	± 16	59
aGNN set 2	0.30	± 0.23	± 0.18	1
aGNN set 3	3.8	± 2.2	± 2.0	5

Table 10. The estimated number of events from the background prediction based on control samples in data and the observed event yields. Statistical and systematic uncertainties in the estimated background are provided.

8 Results

After the full event selection, the observed and expected event yields corresponding to each selection set are shown in table 10. No statistically significant deviation from the SM background prediction is observed. The observation is used to set upper limits on the various signal parameter models considered using the CL_s criterion [63, 64]. The test statistic is defined as the likelihood ratio employed in Higgs boson analyses in ATLAS and CMS, as elaborated in ref. [65]. Upper limits at the 95% confidence level (CL) on the production cross section in the 2-dimensional plane defined by the signal parameters are shown in figures 7 ($m_{\pi_{\text{dark}}} = 10 \text{ GeV}$) and 8 ($m_{\pi_{\text{dark}}} = 20 \text{ GeV}$) for both the unflavored and the flavor-aligned scenarios, and in figure 9 ($m_{\pi_{\text{dark}}} = 6 \text{ GeV}$) for the flavor-aligned scenario. These excluded cross sections are compared to the theoretical prediction to derive the exclusion regions shown as red and black curves for the expected and observed 95% CL limit, respectively. The red curves also have an associated red band to indicate the 68% CL variation on the expected exclusion limit.

In the unflavored coupling model, the key tagging variable for the model-agnostic method is the mean d_{xy} of the associated tracks in the jet. In the case where the dark pion lifetime

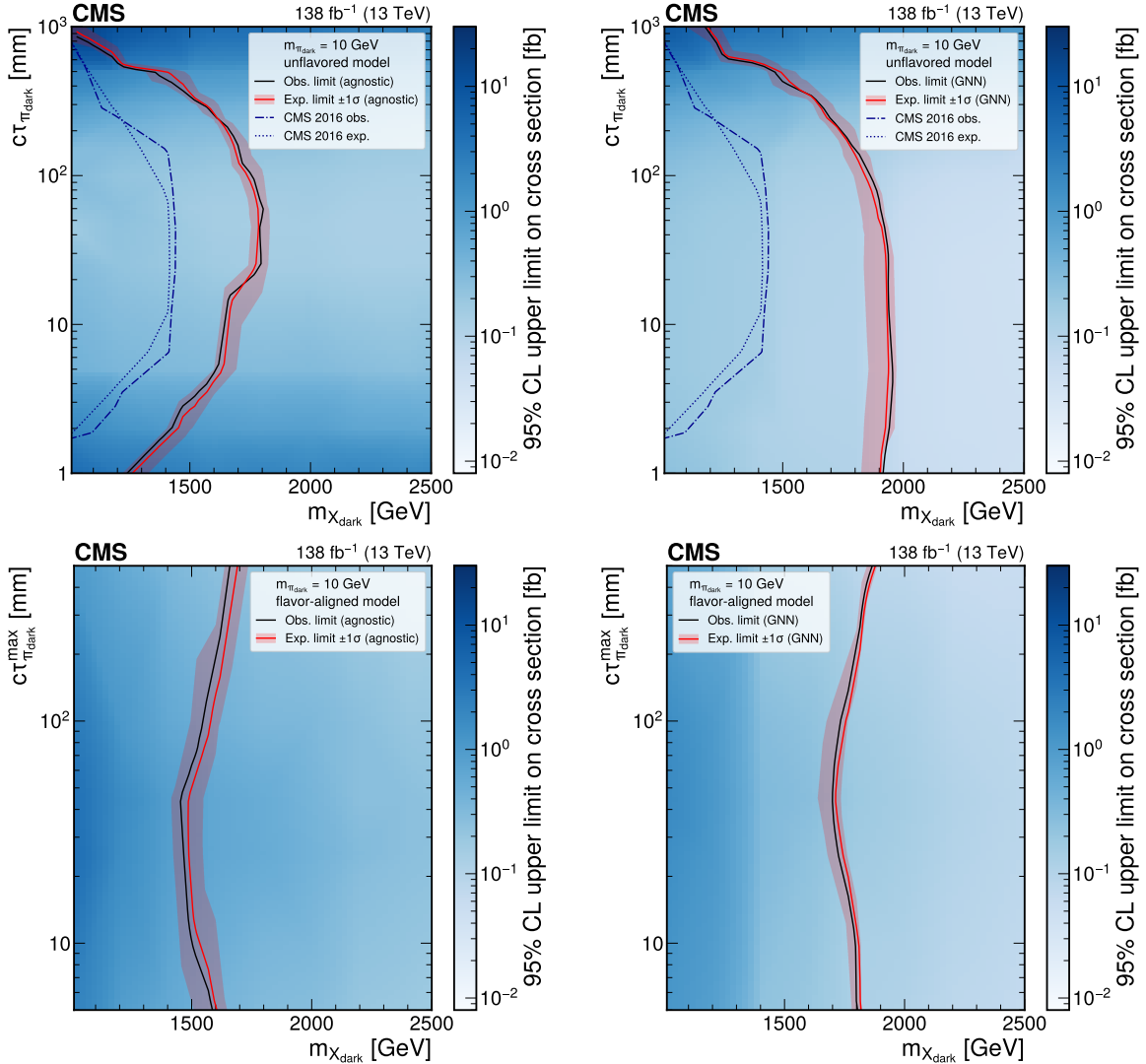


Figure 7. The 95% CL upper limits on the production cross section for various signal models in the unflavored scenario (upper plots) and the flavor-aligned scenario (lower plots) with $m_{\pi_{\text{dark}}} = 10 \text{ GeV}$ using the model-agnostic (GNN) EJ tagging method, on the left (right). The red curve is the expected exclusion limit, with the band representing its 68% CL variation. The black curve is the observed limit. The dark blue dotted curves in the upper plots are the expected and observed limits previously obtained by CMS [21].

is too short, the displaced tracks from the dark pion decay products will be very similar to prompt SM tracks. In the opposite case, where the dark pion lifetime is very large, the dark pions increasingly decay outside the tracker. Thus, this search method is less sensitive to these two cases, giving reduced performance, as shown in the upper-left plots of figures 7 and 8. In contrast, the GNN method performs well even at low dark pion lifetimes, as the GNN leverages information from track-level relationships within EJs to keep the signal acceptance high. However, signal sensitivity is still limited for long dark pion lifetimes, as shown in the upper-right plots of figures 7 and 8.

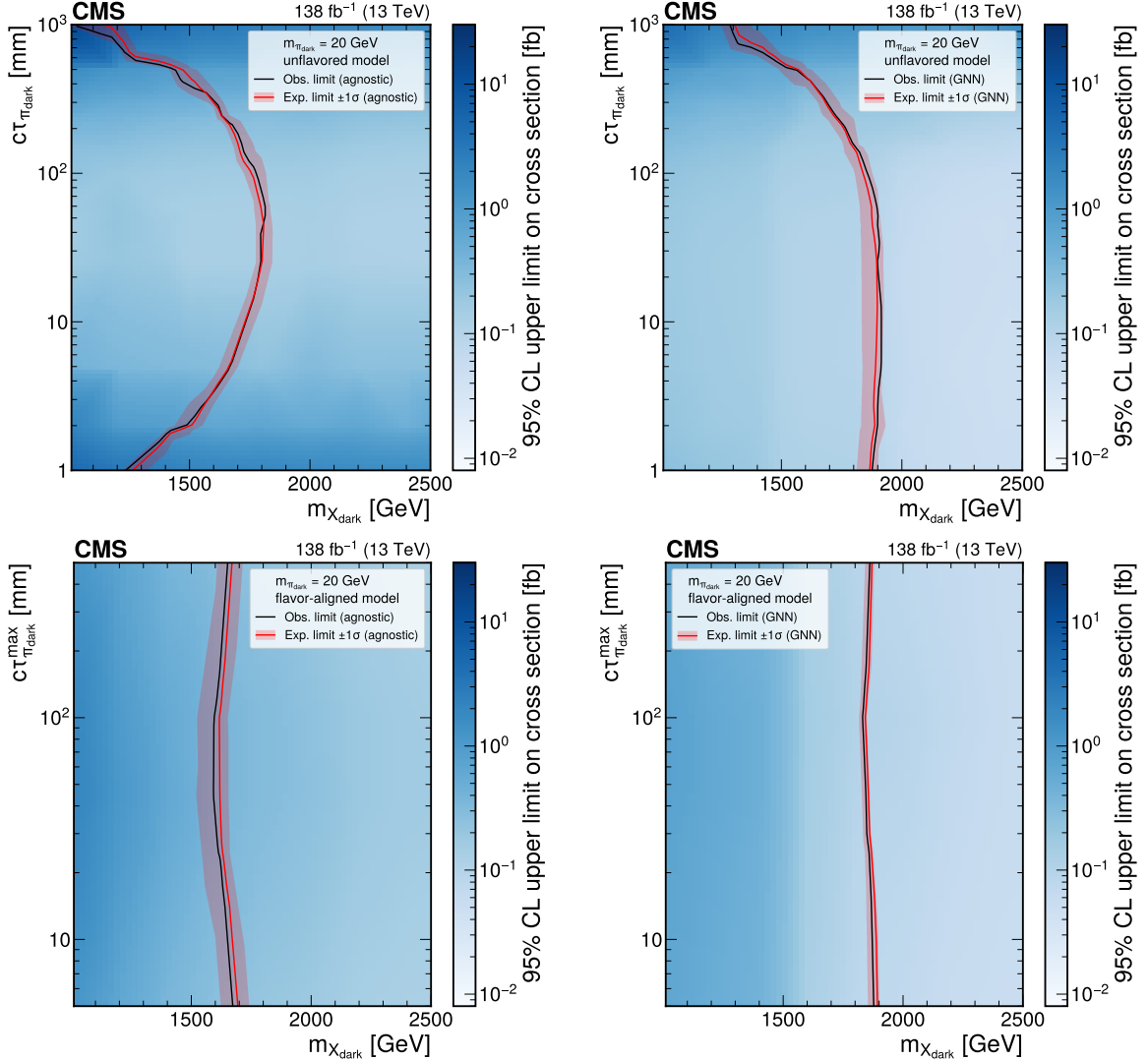


Figure 8. The 95% CL upper limits on the production cross section for various signal models in the unflavored scenario (upper plots) and the flavor-aligned scenario (lower plots) with $m_{\pi_{\text{dark}}} = 20 \text{ GeV}$ using the model-agnostic (GNN) EJ tagging method, on the left (right). The red curve is the expected exclusion limit, with the band representing its 68% CL variation. The black curve is the observed limit.

In the flavor-aligned scenario, the differentiating power for the model-agnostic method comes mainly from the multiplicity of associated tracks with large displacements. Unlike d_{xy} , the multiplicity distribution is more uniform for different dark pion lifetimes (as we only consider $c\tau_{\pi_{\text{dark}}}^{\text{max}}$ above the typical b hadron lifetime) leading to less dependence on $c\tau_{\pi_{\text{dark}}}^{\text{max}}$ as seen in the lower-left plots of figures 7 and 8. Similarly, the GNN sensitivity is less dependent on changes in lifetime, resulting in a stable signal acceptance across the $c\tau_{\pi_{\text{dark}}}^{\text{max}}$ range. In the flavor-aligned models where $m_{\pi_{\text{dark}}} = 6 \text{ GeV}$, the dark pions decay predominantly to light SM quarks because of mass constraints, resulting in fewer displaced tracks in the events. This reduces the selection efficiencies for these signal models, leading to the model-agnostic method having less sensitivity compared to models with larger $m_{\pi_{\text{dark}}}$, as shown in figure 9.

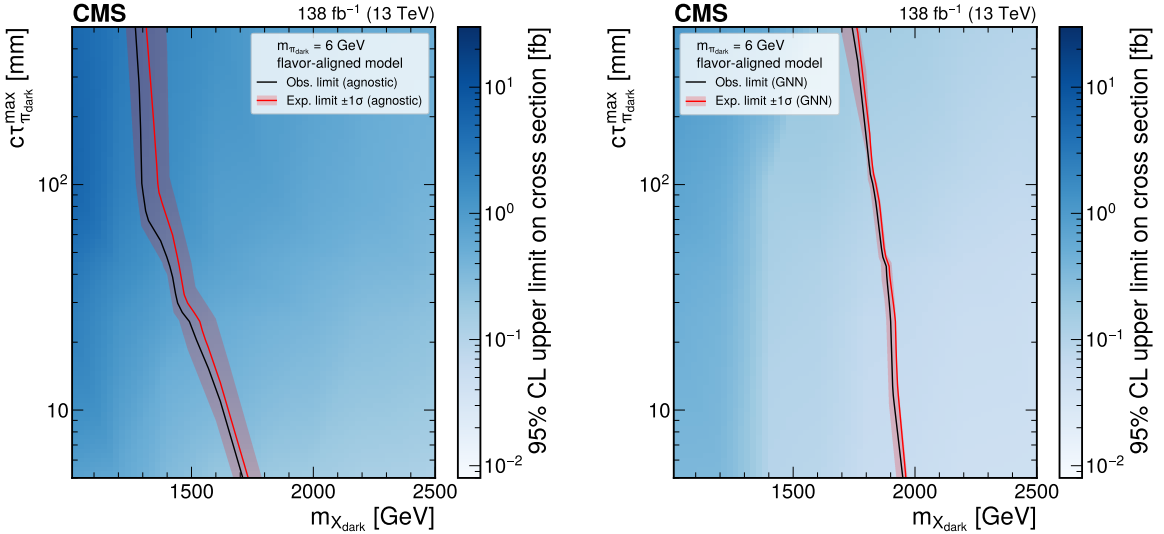


Figure 9. The 95% CL upper limits on the production cross section for various signal models in the flavor-aligned scenario with $m_{\pi_{\text{dark}}} = 6 \text{ GeV}$ using the model-agnostic (GNN) EJ tagging method, on the left (right). The red curve is the expected exclusion limit, with the band representing its 68% CL variation. The black curve is the observed limit.

The ML-based EJ tagging methods yield more stringent limits on the surveyed models. In the unflavored model, X_{dark} masses up to 1900 and 1950 GeV are excluded at 95% CL for $m_{\pi_{\text{dark}}}$ of 10 and 20 GeV, respectively, closely matching the expected limits. For the flavor-aligned models, the X_{dark} mass exclusion at 95% CL increases to 1950, 1850, and 1900 GeV for $m_{\pi_{\text{dark}}}$ of 6, 10, and 20 GeV, respectively, again matching well the expected limits. Relative to the model-agnostic tagger, the greatest increase in sensitivity is for the unflavored signal models with short lifetimes, where the dark showers generate nearly prompt tracks that are difficult to tag using simple requirements on the track displacement variables.

For the flavor-aligned scenario in the model-agnostic approach, the exclusion range on $m_{X_{\text{dark}}}$ initially decreases as $c\tau_{\pi_{\text{dark}}}^{\text{max}}$ increases. This is due to the decline in signal selection efficiency caused by the loss in track reconstruction efficiency, particularly for more displaced tracks. As $c\tau_{\pi_{\text{dark}}}^{\text{max}}$ continues to increase, the displacement of the dark pion with the next longest lifetime, calculated from eq. (1.2), becomes significant for models with $m_{\pi_{\text{dark}}} = 10$ GeV, resulting in a recovery in signal selection efficiency. However, for models with $m_{\pi_{\text{dark}}} = 6$ GeV, the decay of dark pions to $b\bar{b}$ is constrained due to mass limitations. Consequently, the fraction of long-lived dark pions is higher compared to models with $m_{\pi_{\text{dark}}} = 10$ GeV, leading to decreasing signal efficiency even with longer lifetimes.

The GNN-based limits for the flavor-aligned models that utilize the aGNN set 2 selection have a narrow expected band, as shown in the lower right plots of figures 7–8 and the right plot of figure 9. For that selection set, 0.3 background events are predicted, which implies that the most frequent observation will be exactly zero events if the background-only hypothesis is correct. Because the likelihood function is constructed from Poisson probabilities, this leads to the background-only test statistic distribution exhibiting discrete, narrow peaks. With a free-floating signal strength, the test statistic distribution for the signal plus background

hypothesis shares similar features. As a result, only a small change in the signal strength is required to obtain a CL_s value of 0.05 when going from 95 to 68% CL to the expected median of the background expectation. The resulting expected limit bands in this region are narrow and asymmetrical.

9 Summary

A search for emerging jet signatures arising from a strongly interacting dark sector produced in proton-proton collisions has been presented, using data corresponding to an integrated luminosity of 138 fb^{-1} at $\sqrt{s} = 13 \text{ TeV}$. The signal model contains a family of dark quarks that couple to the standard model (SM) quarks via a scalar mediator X_{dark} . Dark pions (π_{dark}) with a significant lifetime ($c\tau_{\pi_{\text{dark}}}$) are produced by the hadronization of the dark quarks; these then decay to SM particles at vertices displaced from the proton-proton interaction point. As the scalar mediator is assumed to be produced in pairs, and each decays to an SM quark and a dark quark, the signature of this process is two SM jets plus two jets of particles with constituents emerging from displaced vertices.

Both unflavored and flavor-aligned couplings between the SM quarks and the dark quarks are examined in the search. Events are selected using either a traditional cut-based approach or a graph neural network to identify emerging jets, in combination with other event-level selection criteria. The overall selection requirements are optimized for each coupling scenario and for different combinations of the mediator particle mass, dark pion mass, and dark pion lifetime. No excess of events beyond the SM expectations is found, and the observed 95% confidence level exclusion limits agree with the expected limits. For the unflavored model, dark mediator masses $m_{X_{\text{dark}}} < 1950 \text{ GeV}$ are excluded for $c\tau_{\pi_{\text{dark}}} \approx 100 \text{ mm}$ and $m_{\pi_{\text{dark}}} = 10 \text{ GeV}$, while the flavor-aligned model result excludes $m_{X_{\text{dark}}} < 1850 \text{ GeV}$ at $c\tau_{\pi_{\text{dark}}}^{\text{max}} \approx 500 \text{ mm}$ for $m_{\pi_{\text{dark}}} = 10 \text{ GeV}$. This result surpasses the previous search for emerging jets in the unflavored scenario, increasing the experimental limit of the dark mediator particle by $\approx 500 \text{ GeV}$ to set the most stringent limits to date, and provides the first direct exclusion of the flavor-aligned scenario.

Acknowledgments

We congratulate our colleagues in the CERN accelerator departments for the excellent performance of the LHC and thank the technical and administrative staffs at CERN and at other CMS institutes for their contributions to the success of the CMS effort. In addition, we gratefully acknowledge the computing centers and personnel of the Worldwide LHC Computing Grid and other centers for delivering so effectively the computing infrastructure essential to our analyses. Finally, we acknowledge the enduring support for the construction and operation of the LHC, the CMS detector, and the supporting computing infrastructure provided by the following funding agencies: SC (Armenia), BMBWF and FWF (Austria); FNRS and FWO (Belgium); CNPq, CAPES, FAPERJ, FAPERGS, and FAPESP (Brazil); MES and BNSF (Bulgaria); CERN; CAS, MoST, and NSFC (China); MINCIENCIAS (Colombia); MSES and CSF (Croatia); RIF (Cyprus); SENESCYT (Ecuador); ERC PRG, RVTT3 and MoER TK202 (Estonia); Academy of Finland, MEC, and HIP (Finland); CEA and CNRS/IN2P3 (France); SRNSF (Georgia); BMBF, DFG, and HGF (Germany); GSRI

(Greece); NKFIH (Hungary); DAE and DST (India); IPM (Iran); SFI (Ireland); INFN (Italy); MSIP and NRF (Republic of Korea); MES (Latvia); LMTLT (Lithuania); MOE and UM (Malaysia); BUAP, CINVESTAV, CONACYT, LNS, SEP, and UASLP-FAI (Mexico); MOS (Montenegro); MBIE (New Zealand); PAEC (Pakistan); MES and NSC (Poland); FCT (Portugal); MESTD (Serbia); MCIN/AEI and PCTI (Spain); MOSTR (Sri Lanka); Swiss Funding Agencies (Switzerland); MST (Taipei); MHESI and NSTDA (Thailand); TUBITAK and TENMAK (Turkey); NASU (Ukraine); STFC (United Kingdom); DOE and NSF (U.S.A.).

Individuals have received support from the Marie-Curie program and the European Research Council and Horizon 2020 Grant, contract Nos. 675440, 724704, 752730, 758316, 765710, 824093, 101115353, and COST Action CA16108 (European Union); the Leventis Foundation; the Alfred P. Sloan Foundation; the Alexander von Humboldt Foundation; the Science Committee, project no. 22rl-037 (Armenia); the Belgian Federal Science Policy Office; the Fonds pour la Formation à la Recherche dans l’Industrie et dans l’Agriculture (FRIA-Belgium); the Agentschap voor Innovatie door Wetenschap en Technologie (IWT-Belgium); the F.R.S.-FNRS and FWO (Belgium) under the “Excellence of Science — EOS” — be.h project n. 30820817; the Beijing Municipal Science & Technology Commission, No. Z191100007219010 and Fundamental Research Funds for the Central Universities (China); the Ministry of Education, Youth and Sports (MEYS) of the Czech Republic; the Shota Rustaveli National Science Foundation, grant FR-22-985 (Georgia); the Deutsche Forschungsgemeinschaft (DFG), under Germany’s Excellence Strategy — EXC 2121 “Quantum Universe” — 390833306, and under project number 400140256 — GRK2497; the Hellenic Foundation for Research and Innovation (HFRI), Project Number 2288 (Greece); the Hungarian Academy of Sciences, the New National Excellence Program — ÚNKP, the NKFIH research grants K 124845, K 124850, K 128713, K 128786, K 129058, K 131991, K 133046, K 138136, K 143460, K 143477, 2020-2.2.1-ED-2021-00181, and TKP2021-NKTA-64 (Hungary); the Council of Science and Industrial Research, India; ICSC — National Research Center for High Performance Computing, Big Data and Quantum Computing, funded by the NextGenerationEU program (Italy); the Latvian Council of Science; the Ministry of Education and Science, project no. 2022/WK/14, and the National Science Center, contracts Opus 2021/41/B/ST2/01369 and 2021/43/B/ST2/01552 (Poland); the Fundação para a Ciência e a Tecnologia, grant CEECIND/01334/2018 (Portugal); the National Priorities Research Program by Qatar National Research Fund; MCIN/AEI/10.13039/501100011033, ERDF “a way of making Europe”, and the Programa Estatal de Fomento de la Investigación Científica y Técnica de Excelencia María de Maeztu, grant MDM-2017-0765 and Programa Severo Ochoa del Principado de Asturias (Spain); the Chulalongkorn Academic into Its 2nd Century Project Advancement Project, and the National Science, Research and Innovation Fund via the Program Management Unit for Human Resources & Institutional Development, Research and Innovation, grant B37G660013 (Thailand); the Kavli Foundation; the Nvidia Corporation; the SuperMicro Corporation; the Welch Foundation, contract C-1845; and the Weston Havens Foundation (U.S.A.).

Open Access. This article is distributed under the terms of the Creative Commons Attribution License ([CC-BY4.0](https://creativecommons.org/licenses/by/4.0/)), which permits any use, distribution and reproduction in any medium, provided the original author(s) and source are credited.

References

- [1] V.C. Rubin, N. Thonnard and W.K. Ford Jr., *Rotational properties of 21 SC galaxies with a large range of luminosities and radii, from NGC 4605 ($R = 4$ kpc) to UGC 2885 ($R = 122$ kpc)*, *Astrophys. J.* **238** (1980) 471 [[INSPIRE](#)].
- [2] M. Persic, P. Salucci and F. Stel, *The universal rotation curve of spiral galaxies: I. The dark matter*, *Mon. Not. Roy. Astron. Soc.* **281** (1996) 27 [[astro-ph/9506004](#)] [[INSPIRE](#)].
- [3] D. Clowe et al., *A direct empirical proof of the existence of dark matter*, *Astrophys. J. Lett.* **648** (2006) L109 [[astro-ph/0608407](#)] [[INSPIRE](#)].
- [4] DES collaboration, *Dark Energy Survey Year 1 results: curved-sky weak lensing mass map*, *Mon. Not. Roy. Astron. Soc.* **475** (2018) 3165 [[arXiv:1708.01535](#)] [[INSPIRE](#)].
- [5] PLANCK collaboration, *Planck 2018 results. VI. Cosmological parameters*, *Astron. Astrophys.* **641** (2020) A6 [*Erratum ibid.* **652** (2021) C4] [[arXiv:1807.06209](#)] [[INSPIRE](#)].
- [6] M.J. Strassler and K.M. Zurek, *Echoes of a hidden valley at hadron colliders*, *Phys. Lett. B* **651** (2007) 374 [[hep-ph/0604261](#)] [[INSPIRE](#)].
- [7] K. Petraki and R.R. Volkas, *Review of asymmetric dark matter*, *Int. J. Mod. Phys. A* **28** (2013) 1330028 [[arXiv:1305.4939](#)] [[INSPIRE](#)].
- [8] H. Beuchesne, E. Bertuzzo and G. Grilli Di Cortona, *Dark matter in Hidden Valley models with stable and unstable light dark mesons*, *JHEP* **04** (2019) 118 [[arXiv:1809.10152](#)] [[INSPIRE](#)].
- [9] Y. Bai and P. Schwaller, *Scale of dark QCD*, *Phys. Rev. D* **89** (2014) 063522 [[arXiv:1306.4676](#)] [[INSPIRE](#)].
- [10] T. Cohen, M. Lisanti and H.K. Lou, *Semivisible jets: dark matter undercover at the LHC*, *Phys. Rev. Lett.* **115** (2015) 171804 [[arXiv:1503.00009](#)] [[INSPIRE](#)].
- [11] P. Schwaller, D. Stolarski and A. Weiler, *Emerging jets*, *JHEP* **05** (2015) 059 [[arXiv:1502.05409](#)] [[INSPIRE](#)].
- [12] P. Agrawal, M. Blanke and K. Gemmler, *Flavored dark matter beyond Minimal Flavor Violation*, *JHEP* **10** (2014) 072 [[arXiv:1405.6709](#)] [[INSPIRE](#)].
- [13] S. Renner and P. Schwaller, *A flavoured dark sector*, *JHEP* **08** (2018) 052 [[arXiv:1803.08080](#)] [[INSPIRE](#)].
- [14] P. Fayet and S. Ferrara, *Supersymmetry*, *Phys. Rept.* **32** (1977) 249 [[INSPIRE](#)].
- [15] C. Borschensky et al., *Squark and gluino production cross sections in pp collisions at $\sqrt{s} = 13, 14, 33$ and 100 TeV*, *Eur. Phys. J. C* **74** (2014) 3174 [[arXiv:1407.5066](#)] [[INSPIRE](#)].
- [16] W. Beenakker et al., *NNLL-fast: predictions for coloured supersymmetric particle production at the LHC with threshold and Coulomb resummation*, *JHEP* **12** (2016) 133 [[arXiv:1607.07741](#)] [[INSPIRE](#)].
- [17] E. Witten, *Baryons in the $1/N$ Expansion*, *Nucl. Phys. B* **160** (1979) 57 [[INSPIRE](#)].
- [18] CMS collaboration, *Search for resonant production of strongly coupled dark matter in proton-proton collisions at 13 TeV*, *JHEP* **06** (2022) 156 [[arXiv:2112.11125](#)] [[INSPIRE](#)].
- [19] ATLAS collaboration, *Search for non-resonant production of semi-visible jets using Run 2 data in ATLAS*, *Phys. Lett. B* **848** (2024) 138324 [[arXiv:2305.18037](#)] [[INSPIRE](#)].
- [20] ATLAS collaboration, *Search for resonant production of dark quarks in the dijet final state with the ATLAS detector*, *JHEP* **02** (2024) 128 [[arXiv:2311.03944](#)] [[INSPIRE](#)].

- [21] CMS collaboration, *Search for new particles decaying to a jet and an emerging jet*, *JHEP* **02** (2019) 179 [[arXiv:1810.10069](#)] [[INSPIRE](#)].
- [22] HEPData record for this analysis, DOI:[10.17182/hepdata.147271](#), (2024).
- [23] CMS collaboration, *Description and performance of track and primary-vertex reconstruction with the CMS tracker*, *2014 JINST* **9** P10009 [[arXiv:1405.6569](#)] [[INSPIRE](#)].
- [24] CMS TRACKER GROUP collaboration, *The CMS Phase-1 pixel detector upgrade*, *2021 JINST* **16** P02027 [[arXiv:2012.14304](#)] [[INSPIRE](#)].
- [25] CMS collaboration, *Track impact parameter resolution for the full pseudo rapidity coverage in the 2017 dataset with the CMS Phase-1 Pixel detector*, CMS-DP-2020-049 (2020).
- [26] CMS collaboration, *Performance of the CMS Level-1 trigger in proton-proton collisions at $\sqrt{s} = 13$ TeV*, *2020 JINST* **15** P10017 [[arXiv:2006.10165](#)] [[INSPIRE](#)].
- [27] CMS collaboration, *The CMS trigger system*, *2017 JINST* **12** P01020 [[arXiv:1609.02366](#)] [[INSPIRE](#)].
- [28] CMS collaboration, *The CMS experiment at the CERN LHC*, *2008 JINST* **3** S08004 [[INSPIRE](#)].
- [29] L. Carloni and T. Sjöstrand, *Visible effects of invisible Hidden Valley radiation*, *JHEP* **09** (2010) 105 [[arXiv:1006.2911](#)] [[INSPIRE](#)].
- [30] L. Carloni, J. Rathsman and T. Sjöstrand, *Discerning secluded sector gauge structures*, *JHEP* **04** (2011) 091 [[arXiv:1102.3795](#)] [[INSPIRE](#)].
- [31] T. Sjöstrand et al., *An introduction to PYTHIA 8.2*, *Comput. Phys. Commun.* **191** (2015) 159 [[arXiv:1410.3012](#)] [[INSPIRE](#)].
- [32] J. Alwall et al., *The automated computation of tree-level and next-to-leading order differential cross sections, and their matching to parton shower simulations*, *JHEP* **07** (2014) 079 [[arXiv:1405.0301](#)] [[INSPIRE](#)].
- [33] J. Alwall et al., *Comparative study of various algorithms for the merging of parton showers and matrix elements in hadronic collisions*, *Eur. Phys. J. C* **53** (2008) 473 [[arXiv:0706.2569](#)] [[INSPIRE](#)].
- [34] CMS collaboration, *Extraction and validation of a new set of CMS PYTHIA8 tunes from underlying-event measurements*, *Eur. Phys. J. C* **80** (2020) 4 [[arXiv:1903.12179](#)] [[INSPIRE](#)].
- [35] NNPDF collaboration, *Parton distributions from high-precision collider data*, *Eur. Phys. J. C* **77** (2017) 663 [[arXiv:1706.00428](#)] [[INSPIRE](#)].
- [36] GEANT4 collaboration, *GEANT4 — a simulation toolkit*, *Nucl. Instrum. Meth. A* **506** (2003) 250 [[INSPIRE](#)].
- [37] CMS collaboration, *Particle-flow reconstruction and global event description with the CMS detector*, *2017 JINST* **12** P10003 [[arXiv:1706.04965](#)] [[INSPIRE](#)].
- [38] CMS collaboration, *Performance of reconstruction and identification of τ leptons decaying to hadrons and ν_τ in pp collisions at $\sqrt{s} = 13$ TeV*, *2018 JINST* **13** P10005 [[arXiv:1809.02816](#)] [[INSPIRE](#)].
- [39] CMS collaboration, *Jet energy scale and resolution in the CMS experiment in pp collisions at 8 TeV*, *2017 JINST* **12** P02014 [[arXiv:1607.03663](#)] [[INSPIRE](#)].
- [40] CMS collaboration, *Performance of missing transverse momentum reconstruction in proton-proton collisions at $\sqrt{s} = 13$ TeV using the CMS detector*, *2019 JINST* **14** P07004 [[arXiv:1903.06078](#)] [[INSPIRE](#)].

- [41] K. Rose, *Deterministic annealing for clustering, compression, classification, regression, and related optimization problems*, *IEEE Proc.* **86** (1998) 2210 [[INSPIRE](#)].
- [42] R. Fruhwirth, W. Waltenberger and P. Vanlaer, *Adaptive vertex fitting*, *J. Phys. G* **34** (2007) N343 [[INSPIRE](#)].
- [43] D. Contardo et al., *Technical Proposal for the Phase-II Upgrade of the CMS Detector*, CERN-LHCC-2015-010 (2015) [[DOI:10.17181/CERN.VU8I.D59J](#)].
- [44] CMS collaboration, *Pileup mitigation at CMS in 13 TeV data*, 2020 *JINST* **15** P09018 [[arXiv:2003.00503](#)] [[INSPIRE](#)].
- [45] M. Cacciari, G.P. Salam and G. Soyez, *The anti- k_t jet clustering algorithm*, *JHEP* **04** (2008) 063 [[arXiv:0802.1189](#)] [[INSPIRE](#)].
- [46] M. Cacciari, G.P. Salam and G. Soyez, *FastJet user manual*, *Eur. Phys. J. C* **72** (2012) 1896 [[arXiv:1111.6097](#)] [[INSPIRE](#)].
- [47] E. Bols et al., *Jet flavour classification using DeepJet*, 2020 *JINST* **15** P12012 [[arXiv:2008.10519](#)] [[INSPIRE](#)].
- [48] CMS collaboration, *Identification of heavy-flavour jets with the CMS detector in pp collisions at 13 TeV*, 2018 *JINST* **13** P05011 [[arXiv:1712.07158](#)] [[INSPIRE](#)].
- [49] CMS collaboration, *Performance summary of AK4 jet b tagging with data from proton-proton collisions at 13 TeV with the CMS detector*, CMS-DP-2023-005 (2023).
- [50] CMS collaboration, *Jet algorithms performance in 13 TeV data*, CMS-PAS-JME-16-003, CERN, Geneva (2017).
- [51] J. Thaler and K. Van Tilburg, *Identifying boosted objects with N-subjettiness*, *JHEP* **03** (2011) 015 [[arXiv:1011.2268](#)] [[INSPIRE](#)].
- [52] H. Qu and L. Gouskos, *Jet tagging via particle clouds*, *Phys. Rev. D* **101** (2020) 056019 [[arXiv:1902.08570](#)] [[INSPIRE](#)].
- [53] C. Savard, *Emerging jets search, Triton server deployment, and track quality development: machine learning applications in high energy physics*, Ph.D. Thesis, University of Colorado, Boulder (2024) [[CERN-THESIS-2024-053](#)] [[INSPIRE](#)].
- [54] CMS collaboration, *Precision luminosity measurement in proton-proton collisions at $\sqrt{s} = 13$ TeV in 2015 and 2016 at CMS*, *Eur. Phys. J. C* **81** (2021) 800 [[arXiv:2104.01927](#)] [[INSPIRE](#)].
- [55] CMS collaboration, *CMS luminosity measurement for the 2017 data-taking period at $\sqrt{s} = 13$ TeV*, CMS-PAS-LUM-17-004, CERN, Geneva (2018).
- [56] CMS collaboration, *CMS luminosity measurement for the 2018 data-taking period at $\sqrt{s} = 13$ TeV*, CMS-PAS-LUM-18-002, CERN, Geneva (2019).
- [57] CMS collaboration, *Measurement of the inelastic proton-proton cross section at $\sqrt{s} = 13$ TeV*, *JHEP* **07** (2018) 161 [[arXiv:1802.02613](#)] [[INSPIRE](#)].
- [58] NNPDF collaboration, *Parton distributions with QED corrections*, *Nucl. Phys. B* **877** (2013) 290 [[arXiv:1308.0598](#)] [[INSPIRE](#)].
- [59] CMS collaboration, *Muon tracking performance in the CMS Run-2 Legacy data using the tag-and-probe technique*, CMS-DP-2020-035 (2020).
- [60] CMS collaboration, *Search for long-lived heavy neutral leptons with displaced vertices in proton-proton collisions at $\sqrt{s} = 13$ TeV*, *JHEP* **07** (2022) 081 [[arXiv:2201.05578](#)] [[INSPIRE](#)].

- [61] M. Cacciari et al., *The $t\bar{t}$ cross-section at 1.8 TeV and 1.96 TeV: A study of the systematics due to parton densities and scale dependence*, *JHEP* **04** (2004) 068 [[hep-ph/0303085](#)] [[inSPIRE](#)].
- [62] S. Catani, D. de Florian, M. Grazzini and P. Nason, *Soft gluon resummation for Higgs boson production at hadron colliders*, *JHEP* **07** (2003) 028 [[hep-ph/0306211](#)] [[inSPIRE](#)].
- [63] T. Junk, *Confidence level computation for combining searches with small statistics*, *Nucl. Instrum. Meth. A* **434** (1999) 435 [[hep-ex/9902006](#)] [[inSPIRE](#)].
- [64] A.L. Read, *Presentation of search results: The CL_s technique*, *J. Phys. G* **28** (2002) 2693 [[inSPIRE](#)].
- [65] ATLAS and CMS collaborations, *Procedure for the LHC Higgs boson search combination in Summer 2011*, [CMS-NOTE-2011-005](#), CERN, Geneva (2011).

The CMS collaboration

Yerevan Physics Institute, Yerevan, Armenia

A. Hayrapetyan, A. Tumasyan¹

Institut für Hochenergiephysik, Vienna, Austria

W. Adam¹, J.W. Andrejkovic, T. Bergauer¹, S. Chatterjee¹, K. Damanakis¹, M. Dragicevic¹, P.S. Hussain¹, M. Jeitler^{1,2}, N. Krammer¹, A. Li¹, D. Liko¹, I. Mikulec¹, J. Schieck^{1,2}, R. Schöfbeck¹, D. Schwarz¹, M. Sonawane¹, S. Templ¹, W. Waltenberger¹, C.-E. Wulz^{1,2}

Universiteit Antwerpen, Antwerpen, Belgium

M.R. Darwish³, T. Janssen¹, P. Van Mechelen¹

Vrije Universiteit Brussel, Brussel, Belgium

N. Breugelmans, J. D'Hondt¹, S. Dansana¹, A. De Moor¹, M. Delcourt¹, F. Heyen, S. Lowette¹, I. Makarenko¹, D. Müller¹, S. Tavernier¹, M. Tytgat^{1,4}, G.P. Van Onsem¹, S. Van Putte¹, D. Vannerom¹

Université Libre de Bruxelles, Bruxelles, Belgium

B. Clerbaux¹, A.K. Das, G. De Lentdecker¹, H. Evard¹, L. Favart¹, P. Gianneios¹, D. Hohov¹, J. Jaramillo¹, A. Khalilzadeh, F.A. Khan¹, K. Lee¹, M. Mahdavikhorrami¹, A. Malara¹, S. Paredes¹, L. Thomas¹, M. Vanden Bemden¹, C. Vander Velde¹, P. Vanlaer¹

Ghent University, Ghent, Belgium

M. De Coen¹, D. Dobur¹, G. Gokbulut¹, Y. Hong¹, J. Knolle¹, L. Lambrecht¹, D. Marckx¹, G. Mestdach, K. Mota Amarilo¹, C. Rendón, A. Samalan, K. Skovpen¹, N. Van Den Bossche¹, J. van der Linden¹, L. Wezenbeek¹

Université Catholique de Louvain, Louvain-la-Neuve, Belgium

A. Benecke¹, A. Bethani¹, G. Bruno¹, C. Caputo¹, J. De Favereau De Jeneret¹, C. Delaere¹, I.S. Donertas¹, A. Giammanco¹, A.O. Guzel¹, Sa. Jain¹, V. Lemaitre, J. Lidrych¹, P. Mastrapasqua¹, T.T. Tran¹, S. Wertz¹

Centro Brasileiro de Pesquisas Fisicas, Rio de Janeiro, Brazil

G.A. Alves¹, E. Coelho¹, C. Hensel¹, T. Menezes De Oliveira¹, A. Moraes¹, P. Rebello Teles¹, M. Soeiro, A. Vilela Pereira^{1,5}

Universidade do Estado do Rio de Janeiro, Rio de Janeiro, Brazil

W.L. Aldá Júnior¹, M. Alves Gallo Pereira¹, M. Barroso Ferreira Filho¹, H. Brandao Malbouisson¹, W. Carvalho¹, J. Chinellato⁶, E.M. Da Costa¹, G.G. Da Silveira^{1,7}, D. De Jesus Damiao¹, S. Fonseca De Souza¹, R. Gomes De Souza, M. Macedo¹, J. Martins^{1,8}, C. Mora Herrera¹, L. Mundim¹, H. Nogima¹, J.P. Pinheiro¹, A. Santoro¹, A. Sznajder¹, M. Thiel¹

Universidade Estadual Paulista, Universidade Federal do ABC, São Paulo, Brazil

C.A. Bernardes⁷, L. Calligaris¹⁰, T.R. Fernandez Perez Tomei¹⁰, E.M. Gregores¹⁰,
I. Maietto Silverio¹⁰, P.G. Mercadante¹⁰, S.F. Novaes¹⁰, B. Orzari¹⁰, Sandra S. Padula¹⁰

Institute for Nuclear Research and Nuclear Energy, Bulgarian Academy of Sciences, Sofia, Bulgaria

A. Aleksandrov¹⁰, G. Antchev¹⁰, R. Hadjiiska¹⁰, P. Iaydjiev¹⁰, M. Misheva¹⁰, M. Shopova¹⁰,
G. Sultanov¹⁰

University of Sofia, Sofia, Bulgaria

A. Dimitrov¹⁰, L. Litov¹⁰, B. Pavlov¹⁰, P. Petkov¹⁰, A. Petrov¹⁰, E. Shumka¹⁰

Instituto De Alta Investigación, Universidad de Tarapacá, Casilla 7 D, Arica, Chile

S. Keshri¹⁰, S. Thakur¹⁰

Beihang University, Beijing, China

T. Cheng¹⁰, T. Javaid¹⁰, L. Yuan¹⁰

Department of Physics, Tsinghua University, Beijing, China

Z. Hu¹⁰, Z. Liang, J. Liu, K. Yi¹⁰^{9,10}

Institute of High Energy Physics, Beijing, China

G.M. Chen¹⁰¹¹, H.S. Chen¹⁰¹¹, M. Chen¹⁰¹¹, F. Iemmi¹⁰, C.H. Jiang, A. Kapoor¹⁰¹², H. Liao¹⁰,
Z.-A. Liu¹⁰¹³, R. Sharma¹⁰¹⁴, J.N. Song¹⁰¹³, J. Tao¹⁰, C. Wang¹⁰¹¹, J. Wang¹⁰, Z. Wang¹⁰¹¹, H. Zhang¹⁰,
J. Zhao¹⁰

State Key Laboratory of Nuclear Physics and Technology, Peking University, Beijing, China

A. Agapitos¹⁰, Y. Ban¹⁰, S. Deng¹⁰, B. Guo, C. Jiang¹⁰, A. Levin¹⁰, C. Li¹⁰, Q. Li¹⁰, Y. Mao,
S. Qian, S.J. Qian¹⁰, X. Qin, X. Sun¹⁰, D. Wang¹⁰, H. Yang, L. Zhang¹⁰, Y. Zhao, C. Zhou¹⁰

Guangdong Provincial Key Laboratory of Nuclear Science and Guangdong-Hong Kong Joint Laboratory of Quantum Matter, South China Normal University, Guangzhou, China

S. Yang¹⁰

Sun Yat-Sen University, Guangzhou, China

Z. You¹⁰

University of Science and Technology of China, Hefei, China

K. Jaffel¹⁰, N. Lu¹⁰

Nanjing Normal University, Nanjing, China

G. Bauer¹⁵, B. Li, J. Zhang¹⁰

Institute of Modern Physics and Key Laboratory of Nuclear Physics and Ion-beam Application (MOE) — Fudan University, Shanghai, China

X. Gao¹⁶

Zhejiang University, Hangzhou, Zhejiang, China

Z. Lin^{ID}, C. Lu^{ID}, M. Xiao^{ID}

Universidad de Los Andes, Bogota, Colombia

C. Avila^{ID}, D.A. Barbosa Trujillo, A. Cabrera^{ID}, C. Florez^{ID}, J. Fraga^{ID}, J.A. Reyes Vega

Universidad de Antioquia, Medellin, Colombia

F. Ramirez^{ID}, M. Rodriguez^{ID}, A.A. Ruales Barbosa, J.D. Ruiz Alvarez^{ID}

University of Split, Faculty of Electrical Engineering, Mechanical Engineering and Naval Architecture, Split, Croatia

D. Giljanovic^{ID}, N. Godinovic^{ID}, D. Lelas^{ID}, A. Sculac^{ID}

University of Split, Faculty of Science, Split, Croatia

M. Kovac^{ID}, A. Petkovic, T. Sculac^{ID}

Institute Rudjer Boskovic, Zagreb, Croatia

P. Bargassa^{ID}, V. Brigljevic^{ID}, B.K. Chitroda^{ID}, D. Ferencek^{ID}, K. Jakovcic, S. Mishra^{ID}, A. Starodumov^{ID}¹⁷, T. Susa^{ID}

University of Cyprus, Nicosia, Cyprus

A. Attikis^{ID}, K. Christoforou^{ID}, A. Hadjigapiou, C. Leonidou, J. Mousa^{ID}, C. Nicolaou, L. Paizanos, F. Ptochos^{ID}, P.A. Razis^{ID}, H. Rykaczewski, H. Saka^{ID}, A. Stepennov^{ID}

Charles University, Prague, Czech Republic

M. Finger^{ID}, M. Finger Jr.^{ID}, A. Kveton^{ID}

Universidad San Francisco de Quito, Quito, Ecuador

E. Carrera Jarrin^{ID}

Academy of Scientific Research and Technology of the Arab Republic of Egypt, Egyptian Network of High Energy Physics, Cairo, Egypt

Y. Assran^{18,19}, B. El-mahdy, S. Elgammal¹⁹

Center for High Energy Physics (CHEP-FU), Fayoum University, El-Fayoum, Egypt

M.A. Mahmoud^{ID}, Y. Mohammed^{ID}

National Institute of Chemical Physics and Biophysics, Tallinn, Estonia

K. Ehataht^{ID}, M. Kadastik, T. Lange^{ID}, S. Nandan^{ID}, C. Nielsen^{ID}, J. Pata^{ID}, M. Raidal^{ID}, L. Tani^{ID}, C. Veelken^{ID}

Department of Physics, University of Helsinki, Helsinki, Finland

H. Kirschenmann^{ID}, K. Osterberg^{ID}, M. Voutilainen^{ID}

Helsinki Institute of Physics, Helsinki, Finland

S. Bharthuar , E. Brücken , F. Garcia , P. Inkaew , K.T.S. Kallonen , R. Kinnunen, T. Lampén , K. Lassila-Perini , S. Lehti , T. Lindén , L. Martikainen , M. Myllymäki , M.m. Rantanen , H. Siikonen , J. Tuominiemi

Lappeenranta-Lahti University of Technology, Lappeenranta, Finland

P. Luukka , H. Petrow 

IRFU, CEA, Université Paris-Saclay, Gif-sur-Yvette, France

M. Besancon , F. Couderc , M. Dejardin , D. Denegri, J.L. Faure, F. Ferri , S. Ganjour , P. Gras , G. Hamel de Monchenault , V. Lohezic , J. Malcles , F. Orlandi , L. Portales , J. Rander, A. Rosowsky , M.Ö. Sahin , A. Savoy-Navarro ²⁰, P. Simkina , M. Titov , M. Tornago

Laboratoire Leprince-Ringuet, CNRS/IN2P3, Ecole Polytechnique, Institut Polytechnique de Paris, Palaiseau, France

F. Beaudette , P. Busson , A. Cappati , C. Charlot , M. Chiusi , F. Damas , O. Davignon , A. De Wit , I.T. Ehle , B.A. Fontana Santos Alves , S. Ghosh , A. Gilbert , R. Granier de Cassagnac , A. Hakimi , B. Harikrishnan , L. Kalipoliti , G. Liu , M. Nguyen , C. Ochando , R. Salerno , J.B. Sauvan , Y. Sirois , E. Vernazza , A. Zabi , A. Zghiche

Université de Strasbourg, CNRS, IPHC UMR 7178, Strasbourg, France

J.-L. Agram , J. Andrea , D. Apparu , D. Bloch , J.-M. Brom , E.C. Chabert , C. Collard , S. Falke , U. Goerlach , R. Haeberle , A.-C. Le Bihan , M. Meena , O. Poncet , G. Saha , M.A. Sessini , P. Van Hove , P. Vaucelle

Institut de Physique des 2 Infinis de Lyon (IP2I), Villeurbanne, France

D. Amram, S. Beauceron , B. Blancon , G. Boudoul , N. Chanon , D. Contardo , P. Depasse , C. Dozen ²², H. El Mamouni, J. Fay , S. Gascon , M. Gouzevitch , C. Greenberg, G. Grenier , B. Ille , E. Jourd'huy, I.B. Laktineh, M. Lethuillier , L. Mirabito, S. Perries, A. Purohit , M. Vander Donckt , P. Verdier , J. Xiao

Georgian Technical University, Tbilisi, Georgia

D. Chokheli , I. Lomidze , Z. Tsamalaidze ¹⁷

RWTH Aachen University, I. Physikalisches Institut, Aachen, Germany

V. Botta , L. Feld , K. Klein , M. Lipinski , D. Meuser , A. Pauls , N. Röwert , M. Teroerde 

RWTH Aachen University, III. Physikalisches Institut A, Aachen, Germany

S. Diekmann , A. Dodonova , N. Eich , D. Eliseev , F. Engelke , J. Erdmann , M. Erdmann , P. Fackeldey , B. Fischer , T. Hebbeker , K. Hoepfner , F. Ivone , A. Jung , M.y. Lee , F. Mausolf , M. Merschmeyer , A. Meyer , S. Mukherjee , D. Noll , F. Nowotny, A. Pozdnyakov , Y. Rath, W. Redjeb , F. Rehm, H. Reithler , V. Sarkisov , A. Schmidt , A. Sharma , J.L. Spah , A. Stein , F. Torres Da Silva De Araujo ²³, S. Wiedenbeck , S. Zaleski

RWTH Aachen University, III. Physikalisches Institut B, Aachen, Germany

C. Dziewok , G. Flügge , T. Kress , A. Nowack , O. Pooth , A. Stahl , T. Ziemons ,
A. Zottz 

Deutsches Elektronen-Synchrotron, Hamburg, Germany

H. Aarup Petersen , M. Aldaya Martin , J. Alimena , S. Amoroso, Y. An , J. Bach ,
S. Baxter , M. Bayatmakou , H. Becerril Gonzalez , O. Behnke , A. Belvedere ,
S. Bhattacharya , F. Blekman ²⁴, K. Borras ²⁵, A. Campbell , A. Cardini , C. Cheng,
F. Colombina , S. Consuegra Rodríguez , G. Correia Silva , M. De Silva , G. Eckerlin,
D. Eckstein , L.I. Estevez Banos , O. Filatov , E. Gallo ²⁴, A. Geiser , V. Guglielmi ,
M. Guthoff , A. Hinzmann , L. Jeppe , B. Kaeche , M. Kasemann , C. Kleinwort ,
R. Kogler , M. Komm , D. Krücker , W. Lange, D. Leyva Pernia , K. Lipka ²⁶,
W. Lohmann , F. Lorkowski , R. Mankel , I.-A. Melzer-Pellmann , M. Mendizabal Morentin ,
A.B. Meyer , G. Milella , K. Moral Figueroa , A. Mussgiller , L.P. Nair , J. Niedziela ,
A. Nürnberg , Y. Otari, J. Park , D. Pérez Adán , E. Ranken , A. Raspereza ,
D. Rastorguev , J. Rübenach, L. Rygaard, A. Saggio , M. Scham ^{28,25}, S. Schnake ²⁵,
P. Schütze , C. Schwanenberger ²⁴, D. Selivanova , K. Sharko , M. Shchedrolosiev ,
D. Stafford, F. Vazzoler , A. Ventura Barroso , R. Walsh , D. Wang , Q. Wang , Y. Wen ,
K. Wichmann, L. Wiens , C. Wissing , Y. Yang , A. Zimermann Castro Santos 

University of Hamburg, Hamburg, Germany

A. Albrecht , S. Albrecht , M. Antonello , S. Bein , L. Benato , S. Bollweg, M. Bonanomi ,
P. Connor , K. El Morabit , Y. Fischer , E. Garutti , A. Grohsjean , J. Haller ,
H.R. Jabusch , G. Kasieczka , P. Keicher, R. Klanner , W. Korcari , T. Kramer , C.c. Kuo,
V. Kutzner , F. Labe , J. Lange , A. Lobanov , C. Matthies , L. Moureaux , M. Mrowietz,
A. Nigamova , Y. Nissan, A. Paasch , K.J. Pena Rodriguez , T. Quadfasel , B. Raciti ,
M. Rieger , D. Savoiu , J. Schindler , P. Schleper , M. Schröder , J. Schwandt ,
M. Sommerhalder , H. Stadie , G. Steinbrück , A. Tews, M. Wolf 

Karlsruhe Institut fuer Technologie, Karlsruhe, Germany

S. Brommer , M. Burkart, E. Butz , T. Chwalek , A. Dierlamm , A. Droll, N. Faltermann ,
M. Giffels , A. Gottmann , F. Hartmann ²⁹, R. Hofsaess , M. Horzela , U. Husemann ,
J. Kieseler , M. Klute , R. Koppenhöfer , J.M. Lawhorn , M. Link, A. Lintuluoto ,
B. Maier , S. Maier , S. Mitra , M. Mormile , Th. Müller , M. Neukum, M. Oh ,
E. Pfeffer , M. Presilla , G. Quast , K. Rabbertz , B. Regnery , N. Shadskiy , I. Shvetsov ,
H.J. Simonis , L. Sowa, L. Stockmeier, K. Tauqueer, M. Toms , N. Trevisani , R.F. Von Cube ,
M. Wassmer , S. Wieland , F. Wittig, R. Wolf , X. Zuo 

Institute of Nuclear and Particle Physics (INPP), NCSR Demokritos, Aghia Paraskevi, Greece

G. Anagnostou, G. Daskalakis , A. Kyriakis, A. Papadopoulos²⁹, A. Stakia 

National and Kapodistrian University of Athens, Athens, Greece

P. Kontaxakis , G. Melachroinos, Z. Painesis , A. Panagiotou, I. Papavergou , I. Paraskevas ,
N. Saoulidou , K. Theofilatos , E. Tziaferi , K. Vellidis , I. Zisopoulos 

National Technical University of Athens, Athens, Greece

G. Bakas , T. Chatzistavrou, G. Karapostoli , K. Kousouris , I. Papakrivopoulos ,
E. Siamarkou, G. Tsipolitis, A. Zacharopoulou

University of Ioánnina, Ioánnina, Greece

K. Adamidis, I. Bestintzanos, I. Evangelou , C. Foudas, C. Kamtsikis, P. Katsoulis, P. Kokkas ,
P.G. Kosmoglou Kiouseoglou , N. Manthos , I. Papadopoulos , J. Strologas 

HUN-REN Wigner Research Centre for Physics, Budapest, Hungary

M. Bartók ³⁰, C. Hajdu , D. Horvath ^{31,32}, K. Márton, A.J. Rádl ³³, F. Sikler ,
V. Veszpremi 

MTA-ELTE Lendület CMS Particle and Nuclear Physics Group, Eötvös Loránd University, Budapest, Hungary

M. Csand , K. Farkas , A. Fehrkuti ³⁴, M.M.A. Gadallah , . Kadlecik , P. Major ,
G. Pasztor , G.I. Veres 

Faculty of Informatics, University of Debrecen, Debrecen, Hungary

P. Raics, B. Ujvari , G. Zilizi 

Institute of Nuclear Research ATOMKI, Debrecen, Hungary

G. Bencze, S. Czellar, J. Molnar, Z. Szillasi

Karoly Robert Campus, MATE Institute of Technology, Gyongyos, Hungary

T. Csorgo ³⁴, T. Novak 

Panjab University, Chandigarh, India

J. Babbar , S. Bansal , S.B. Beri, V. Bhatnagar , G. Chaudhary , S. Chauhan ,
N. Dhingra ³⁶, A. Kaur , A. Kaur , H. Kaur , M. Kaur , S. Kumar , K. Sandeep ,
T. Sheokand, J.B. Singh , A. Singla 

University of Delhi, Delhi, India

A. Ahmed , A. Bhardwaj , A. Chhetri , B.C. Choudhary , A. Kumar , A. Kumar ,
M. Naimuddin , K. Ranjan , M.K. Saini, S. Saumya 

Saha Institute of Nuclear Physics, HBNI, Kolkata, India

S. Baradia , S. Barman ³⁷, S. Bhattacharya , S. Das Gupta, S. Dutta , S. Dutta, S. Sarkar

Indian Institute of Technology Madras, Madras, India

M.M. Ameen , P.K. Behera , S.C. Behera , S. Chatterjee , G. Dash , P. Jana , P. Kalbhor ,
S. Kamble , J.R. Komaragiri ³⁸, D. Kumar ³⁸, P.R. Pujahari , N.R. Saha , A. Sharma ,
A.K. Sikdar , R.K. Singh, P. Verma, S. Verma , A. Vijay

Tata Institute of Fundamental Research-A, Mumbai, India

S. Dugad, M. Kumar , G.B. Mohanty , B. Parida , M. Shelake, P. Suryadevara

Tata Institute of Fundamental Research-B, Mumbai, India

A. Bala , S. Banerjee , R.M. Chatterjee, M. Guchait , Sh. Jain , A. Jaiswal, S. Kumar ,
G. Majumder , K. Mazumdar , S. Parolia , A. Thachayath 

National Institute of Science Education and Research, An OCC of Homi Bhabha National Institute, Bhubaneswar, Odisha, India

S. Bahinipati ³⁹, C. Kar , D. Maity ⁴⁰, P. Mal , T. Mishra ,
V.K. Muraleedharan Nair Bindhu , K. Naskar ⁴⁰, A. Nayak ⁴⁰, S. Nayak, K. Pal, P. Sadangi,
S.K. Swain , S. Varghese ⁴⁰, D. Vats ⁴⁰

Indian Institute of Science Education and Research (IISER), Pune, India

S. Acharya ⁴¹, A. Alpana , S. Dube , B. Gomber ⁴¹, P. Hazarika , B. Kansal , A. Laha ,
B. Sahu ⁴¹, S. Sharma , K.Y. Vaish

Isfahan University of Technology, Isfahan, Iran

H. Bakhshiansohi ⁴², A. Jafari ⁴³, M. Zeinali ⁴⁴

Institute for Research in Fundamental Sciences (IPM), Tehran, Iran

S. Bashiri, S. Chenarani ⁴⁵, S.M. Etesami , Y. Hosseini , M. Khakzad , E. Khazaie ⁴⁶,
M. Mohammadi Najafabadi , S. Tizchang 

University College Dublin, Dublin, Ireland

M. Felcini , M. Grunewald 

INFN Sezione di Bari^a, Università di Bari^b, Politecnico di Bari^c, Bari, Italy

M. Abbrescia ^{a,b}, A. Colaleo ^{a,b}, D. Creanza ^{a,c}, B. D'Anzi ^{a,b}, N. De Filippis ^{a,c},
M. De Palma ^{a,b}, A. Di Florio ^{a,c}, L. Fiore ^a, G. Iaselli ^{a,c}, M. Louka ^{a,b}, G. Maggi ^{a,c},
M. Maggi ^a, I. Margjeka ^{a,b}, V. Mastrapasqua ^{a,b}, S. My ^{a,b}, S. Nuzzo ^{a,b}, A. Pellecchia ^{a,b},
A. Pompili ^{a,b}, G. Pugliese ^{a,c}, R. Radogna ^a, D. Ramos ^a, A. Ranieri ^a, L. Silvestris ^a,
F.M. Simone ^{a,b}, Ü. Sözbilir ^a, A. Stamerra ^a, D. Troiano ^a, R. Venditti ^a, P. Verwilligen ^a,
A. Zaza ^{a,b}

INFN Sezione di Bologna^a, Università di Bologna^b, Bologna, Italy

G. Abbiendi ^a, C. Battilana ^{a,b}, D. Bonacorsi ^{a,b}, L. Borgonovi ^a, P. Capiluppi ^{a,b},
A. Castro ^{†,a,b}, F.R. Cavallo ^a, M. Cuffiani ^{a,b}, G.M. Dallavalle ^a, T. Diotalevi ^{a,b},
F. Fabbri ^a, A. Fanfani ^{a,b}, D. Fasanella ^{a,b}, P. Giacomelli ^a, L. Giommi ^{a,b}, C. Grandi ^a,
L. Guiducci ^{a,b}, S. Lo Meo ^{a,47}, M. Lorusso ^{a,b}, L. Lunerti ^a, S. Marcellini ^a, G. Masetti ^a,
F.L. Navarria ^{a,b}, G. Paggi ^a, A. Perrotta ^a, F. Primavera ^{a,b}, A.M. Rossi ^{a,b},
S. Rossi Tisbeni ^{a,b}, T. Rovelli ^{a,b}, G.P. Siroli ^{a,b}

INFN Sezione di Catania^a, Università di Catania^b, Catania, Italy

S. Costa ^{a,b,48}, A. Di Mattia ^a, R. Potenza ^{a,b}, A. Tricomi ^{a,b,48}, C. Tuve ^{a,b}

INFN Sezione di Firenze^a, Università di Firenze^b, Firenze, Italy

P. Assiouras ^a, G. Barbagli ^a, G. Bardelli ^{a,b}, B. Camaiani ^{a,b}, A. Cassese ^a, R. Ceccarelli ^a,
V. Ciulli ^{a,b}, C. Civinini ^a, R. D'Alessandro ^{a,b}, E. Focardi ^{a,b}, T. Kello ^a, G. Latino ^{a,b},

P. Lenzi $\text{ID}^{a,b}$, M. Lizzo ID^a , M. Meschini ID^a , S. Paoletti ID^a , A. Papanastassiou a,b , G. Sguazzoni ID^a , L. Viliani ID^a

INFN Laboratori Nazionali di Frascati, Frascati, Italy

L. Benussi ID , S. Bianco ID , S. Meola ID^{49} , D. Piccolo ID

INFN Sezione di Genova^a, Università di Genova^b, Genova, Italy

P. Chatagnon ID^a , F. Ferro ID^a , E. Robutti ID^a , S. Tosi $\text{ID}^{a,b}$

INFN Sezione di Milano-Bicocca^a, Università di Milano-Bicocca^b, Milano, Italy

A. Benaglia ID^a , G. Boldrini $\text{ID}^{a,b}$, F. Brivio ID^a , F. Cetorelli ID^a , F. De Guio $\text{ID}^{a,b}$, M.E. Dinardo $\text{ID}^{a,b}$, P. Dini ID^a , S. Gennai ID^a , R. Gerosa $\text{ID}^{a,b}$, A. Ghezzi $\text{ID}^{a,b}$, P. Govoni $\text{ID}^{a,b}$, L. Guzzi ID^a , M.T. Lucchini $\text{ID}^{a,b}$, M. Malberti ID^a , S. Malvezzi ID^a , A. Massironi ID^a , D. Menasce ID^a , L. Moroni ID^a , M. Paganoni $\text{ID}^{a,b}$, S. Palluotto $\text{ID}^{a,b}$, D. Pedrini ID^a , A. Perego ID^a , B.S. Pinolini ID^a , G. Pizzati a,b , S. Ragazzi $\text{ID}^{a,b}$, T. Tabarelli de Fatis $\text{ID}^{a,b}$

INFN Sezione di Napoli^a, Università di Napoli ‘Federico II’^b, Napoli, Italy; Università della Basilicata^c, Potenza, Italy; Scuola Superiore Meridionale (SSM)^d, Napoli, Italy

S. Buontempo ID^a , A. Cagnotta $\text{ID}^{a,b}$, F. Carnevali a,b , N. Cavallo $\text{ID}^{a,c}$, F. Fabozzi $\text{ID}^{a,c}$, A.O.M. Iorio $\text{ID}^{a,b}$, L. Lista $\text{ID}^{a,b,50}$, P. Paolucci $\text{ID}^{a,29}$, B. Rossi ID^a , C. Sciacca $\text{ID}^{a,b}$

INFN Sezione di Padova^a, Università di Padova^b, Padova, Italy; Università di Trento^c, Trento, Italy

R. Ardino ID^a , P. Azzi ID^a , N. Bacchetta $\text{ID}^{a,51}$, M. Bellato ID^a , D. Bisello $\text{ID}^{a,b}$, P. Bortignon ID^a , G. Bortolato a,b , A. Bragagnolo $\text{ID}^{a,b}$, A.C.M. Bulla ID^a , R. Carlin $\text{ID}^{a,b}$, P. Checchia ID^a , T. Dorigo ID^a , F. Gasparini $\text{ID}^{a,b}$, U. Gasparini $\text{ID}^{a,b}$, E. Lusiani ID^a , M. Margoni $\text{ID}^{a,b}$, M. Migliorini $\text{ID}^{a,b}$, J. Pazzini $\text{ID}^{a,b}$, P. Ronchese $\text{ID}^{a,b}$, R. Rossin $\text{ID}^{a,b}$, F. Simonetto $\text{ID}^{a,b}$, G. Strong ID^a , M. Tosi $\text{ID}^{a,b}$, A. Triossi $\text{ID}^{a,b}$, S. Ventura ID^a , M. Zanetti $\text{ID}^{a,b}$, P. Zotto $\text{ID}^{a,b}$, A. Zucchetta $\text{ID}^{a,b}$, G. Zumerle $\text{ID}^{a,b}$

INFN Sezione di Pavia^a, Università di Pavia^b, Pavia, Italy

C. Aimè ID^a , A. Braghieri ID^a , S. Calzaferri ID^a , D. Fiorina ID^a , P. Montagna $\text{ID}^{a,b}$, V. Re ID^a , C. Riccardi $\text{ID}^{a,b}$, P. Salvini ID^a , I. Vai $\text{ID}^{a,b}$, P. Vitulo $\text{ID}^{a,b}$

INFN Sezione di Perugia^a, Università di Perugia^b, Perugia, Italy

S. Ajmal $\text{ID}^{a,b}$, M.E. Ascoli a,b , G.M. Bilei ID^a , C. Carrivale a,b , D. Ciangottini $\text{ID}^{a,b}$, L. Fanò $\text{ID}^{a,b}$, M. Magherini $\text{ID}^{a,b}$, V. Mariani $\text{ID}^{a,b}$, M. Menichelli ID^a , F. Moscatelli $\text{ID}^{a,52}$, A. Rossi $\text{ID}^{a,b}$, A. Santocchia $\text{ID}^{a,b}$, D. Spiga ID^a , T. Tedeschi $\text{ID}^{a,b}$

INFN Sezione di Pisa^a, Università di Pisa^b, Scuola Normale Superiore di Pisa^c, Pisa, Italy; Università di Siena^d, Siena, Italy

C.A. Alexe $\text{ID}^{a,c}$, P. Asenov $\text{ID}^{a,b}$, P. Azzurri ID^a , G. Bagliesi ID^a , R. Bhattacharya ID^a , L. Bianchini $\text{ID}^{a,b}$, T. Boccali ID^a , E. Bossini ID^a , D. Bruschini $\text{ID}^{a,c}$, R. Castaldi ID^a , M.A. Ciocci $\text{ID}^{a,b}$, M. Cipriani $\text{ID}^{a,b}$, V. D’Amante $\text{ID}^{a,d}$, R. Dell’Orso ID^a , S. Donato ID^a , A. Giassi ID^a , F. Ligabue $\text{ID}^{a,c}$, D. Matos Figueiredo ID^a , A. Messineo $\text{ID}^{a,b}$, M. Musich $\text{ID}^{a,b}$, F. Palla ID^a , A. Rizzi $\text{ID}^{a,b}$,

G. Rolandi ^{a,c}, S. Roy Chowdhury ^a, T. Sarkar ^a, A. Scribano ^a, P. Spagnolo ^a, R. Tenchini ^a, G. Tonelli ^{a,b}, N. Turini ^{a,d}, F. Vaselli ^{a,c}, A. Venturi ^a, P.G. Verdini ^a

INFN Sezione di Roma^a, Sapienza Università di Roma^b, Roma, Italy

C. Baldenegro Barrera ^{a,b}, P. Barria ^a, C. Basile ^{a,b}, M. Campana ^{a,b}, F. Cavallari ^a, L. Cunqueiro Mendez ^{a,b}, D. Del Re ^{a,b}, E. Di Marco ^a, M. Diemoz ^a, F. Errico ^{a,b}, E. Longo ^{a,b}, P. Meridiani ^a, J. Mijuskovic ^{a,b}, G. Organtini ^{a,b}, F. Pandolfi ^a, R. Paramatti ^{a,b}, C. Quaranta ^{a,b}, S. Rahatlou ^{a,b}, C. Rovelli ^a, F. Santanastasio ^{a,b}, L. Soffi ^a

INFN Sezione di Torino^a, Università di Torino^b, Torino, Italy; Università del Piemonte Orientale^c, Novara, Italy

N. Amapane ^{a,b}, R. Arcidiacono ^{a,c}, S. Argiro ^{a,b}, M. Arneodo ^{a,c}, N. Bartosik ^a, R. Bellan ^{a,b}, A. Bellora ^{a,b}, C. Biino ^a, C. Borca ^{a,b}, N. Cartiglia ^a, M. Costa ^{a,b}, R. Covarelli ^{a,b}, N. Demaria ^a, L. Finco ^a, M. Grippo ^{a,b}, B. Kiani ^{a,b}, F. Legger ^a, F. Luongo ^{a,b}, C. Mariotti ^a, L. Markovic ^{a,b}, S. Maselli ^a, A. Mecca ^{a,b}, L. Menzio ^{a,b}, E. Migliore ^{a,b}, M. Monteno ^a, R. Mulargia ^a, M.M. Obertino ^{a,b}, G. Ortona ^a, L. Pacher ^{a,b}, N. Pastrone ^a, M. Pelliccioni ^a, M. Ruspa ^{a,c}, F. Siviero ^{a,b}, V. Sola ^{a,b}, A. Solano ^{a,b}, A. Staiano ^a, C. Tarricone ^{a,b}, D. Trocino ^a, G. Umoret ^{a,b}, E. Vlasov ^{a,b}, R. White ^{a,b}

INFN Sezione di Trieste^a, Università di Trieste^b, Trieste, Italy

S. Belforte ^a, V. Candelise ^{a,b}, M. Casarsa ^a, F. Cossutti ^a, K. De Leo ^a, G. Della Ricca ^{a,b}

Kyungpook National University, Daegu, Korea

S. Dogra  , J. Hong  , C. Huh  , B. Kim  , J. Kim, D. Lee, H. Lee, S.W. Lee  , C.S. Moon  , Y.D. Oh  , M.S. Ryu  , S. Sekmen , B. Tae, Y.C. Yang

Department of Mathematics and Physics — GWNU, Gangneung, Korea

M.S. Kim 

Chonnam National University, Institute for Universe and Elementary Particles, Kwangju, Korea

G. Bak  , P. Gwak  , H. Kim  , D.H. Moon 

Hanyang University, Seoul, Korea

E. Asilar  , J. Choi  , D. Kim  , T.J. Kim  , J.A. Merlin, Y. Ryou

Korea University, Seoul, Korea

S. Choi  , S. Han, B. Hong  , K. Lee, K.S. Lee  , S. Lee  , S.K. Park, J. Yoo 

Kyung Hee University, Department of Physics, Seoul, Korea

J. Goh  , S. Yang 

Sejong University, Seoul, Korea

H. S. Kim  , Y. Kim, S. Lee

Seoul National University, Seoul, Korea

J. Almond, J.H. Bhyun, J. Choi[✉], J. Choi, W. Jun[✉], J. Kim[✉], S. Ko[✉], H. Kwon[✉], H. Lee[✉], J. Lee[✉], J. Lee[✉], B.H. Oh[✉], S.B. Oh[✉], H. Seo[✉], U.K. Yang, I. Yoon[✉]

University of Seoul, Seoul, Korea

W. Jang[✉], D.Y. Kang, Y. Kang[✉], S. Kim[✉], B. Ko, J.S.H. Lee[✉], Y. Lee[✉], I.C. Park[✉], Y. Roh, I.J. Watson[✉]

Yonsei University, Department of Physics, Seoul, Korea

S. Ha[✉], H.D. Yoo[✉]

Sungkyunkwan University, Suwon, Korea

M. Choi[✉], M.R. Kim[✉], H. Lee, Y. Lee[✉], I. Yu[✉]

College of Engineering and Technology, American University of the Middle East (AUM), Dasman, Kuwait

T. Beyrouthy

Riga Technical University, Riga, Latvia

K. Dreimanis[✉], A. Gaile[✉], G. Pikurs, A. Potrebko[✉], M. Seidel[✉], D. Sidiropoulos Kontos

University of Latvia (LU), Riga, Latvia

N.R. Strautnieks[✉]

Vilnius University, Vilnius, Lithuania

M. Ambrozas[✉], A. Juodagalvis[✉], A. Rinkevicius[✉], G. Tamulaitis[✉]

National Centre for Particle Physics, Universiti Malaya, Kuala Lumpur, Malaysia

N. Bin Norjoharuddeen[✉], I. Yusuff[✉]⁵³, Z. Zolkapli

Universidad de Sonora (UNISON), Hermosillo, Mexico

J.F. Benitez[✉], A. Castaneda Hernandez[✉], H.A. Encinas Acosta, L.G. Gallegos Maríñez, M. León Coello[✉], J.A. Murillo Quijada[✉], A. Sehrawat[✉], L. Valencia Palomo[✉]

Centro de Investigacion y de Estudios Avanzados del IPN, Mexico City, Mexico

G. Ayala[✉], H. Castilla-Valdez[✉], H. Crotte Ledesma, E. De La Cruz-Burelo[✉], I. Heredia-De La Cruz[✉]⁵⁴, R. Lopez-Fernandez[✉], J. Mejia Guisao[✉], C.A. Mondragon Herrera, A. Sánchez Hernández[✉]

Universidad Iberoamericana, Mexico City, Mexico

C. Oropeza Barrera[✉], D.L. Ramirez Guadarrama, M. Ramírez García[✉]

Benemerita Universidad Autonoma de Puebla, Puebla, Mexico

I. Bautista[✉], I. Pedraza[✉], H.A. Salazar Ibarguen[✉], C. Uribe Estrada[✉]

University of Montenegro, Podgorica, Montenegro

I. Bubanja, N. Raicevic[✉]

University of Canterbury, Christchurch, New ZealandP.H. Butler **National Centre for Physics, Quaid-I-Azam University, Islamabad, Pakistan**A. Ahmad , M.I. Asghar, A. Awais , M.I.M. Awan, H.R. Hoorani , W.A. Khan **AGH University of Krakow, Faculty of Computer Science, Electronics and Telecommunications, Krakow, Poland**V. Avati, L. Grzanka , M. Malawski **National Centre for Nuclear Research, Swierk, Poland**H. Bialkowska , M. Bluj , M. Górski , M. Kazana , M. Szleper , P. Zalewski **Institute of Experimental Physics, Faculty of Physics, University of Warsaw, Warsaw, Poland**K. Bunkowski , K. Doroba , A. Kalinowski , M. Konecki , J. Krolikowski , A. Muhammad **Warsaw University of Technology, Warsaw, Poland**K. Pozniak , W. Zabolotny **Laboratório de Instrumentação e Física Experimental de Partículas, Lisboa, Portugal**M. Araujo , D. Bastos , C. Beirão Da Cruz E Silva , A. Boletti , M. Bozzo , T. Camporesi , G. Da Molin , P. Faccioli , M. Gallinaro , J. Hollar , N. Leonardo , G.B. Marozzo, T. Niknejad , A. Petrilli , M. Pisano , J. Seixas , J. Varela , J.W. Wulff**Faculty of Physics, University of Belgrade, Belgrade, Serbia**P. Adzic , P. Milenovic **VINCA Institute of Nuclear Sciences, University of Belgrade, Belgrade, Serbia**M. Dordevic , J. Milosevic , L. Nadderd , V. Rekovic**Centro de Investigaciones Energéticas Medioambientales y Tecnológicas (CIEMAT), Madrid, Spain**J. Alcaraz Maestre , Cristina F. Bedoya , Oliver M. Carretero , M. Cepeda , M. Cerrada , N. Colino , B. De La Cruz , A. Delgado Peris , A. Escalante Del Valle , D. Fernández Del Val , J.P. Fernández Ramos , J. Flix , M.C. Fouz , O. Gonzalez Lopez , S. Goy Lopez , J.M. Hernandez , M.I. Josa , E. Martin Viscasillas , D. Moran , C. M. Morcillo Perez , Á. Navarro Tobar , C. Perez Dengra , A. Pérez-Calero Yzquierdo , J. Puerta Pelayo , I. Redondo , S. Sánchez Navas , J. Sastre , L. Urda Gómez , J. Vazquez Escobar **Universidad Autónoma de Madrid, Madrid, Spain**J.F. de Trocóniz **Universidad de Oviedo, Instituto Universitario de Ciencias y Tecnologías Espaciales de Asturias (ICTEA), Oviedo, Spain**B. Alvarez Gonzalez , J. Cuevas , J. Fernandez Menendez , S. Folgueras , I. Gonzalez Caballero , J.R. González Fernández , P. Leguina , E. Palencia Cortezon 

C. Ramón Álvarez , V. Rodríguez Bouza , A. Soto Rodríguez , A. Trapote , C. Vico Villalba , P. Vischia

Instituto de Física de Cantabria (IFCA), CSIC-Universidad de Cantabria, Santander, Spain

S. Bhowmik , S. Blanco Fernández , J.A. Brochero Cifuentes , I.J. Cabrillo , A. Calderon , J. Duarte Campderros , M. Fernandez , G. Gomez , C. Lasosa García , R. Lopez Ruiz , C. Martinez Rivero , P. Martinez Ruiz del Arbol , F. Matorras , P. Matorras Cuevas , E. Navarrete Ramos , J. Piedra Gomez , L. Scodellaro , I. Vila , J.M. Vizan Garcia

University of Colombo, Colombo, Sri Lanka

B. Kailasapathy ⁵⁵, D.D.C. Wickramarathna

University of Ruhuna, Department of Physics, Matara, Sri Lanka

W.G.D. Dharmaratna ⁵⁶, K. Liyanage , N. Perera

CERN, European Organization for Nuclear Research, Geneva, Switzerland

D. Abbaneo , C. Amendola , E. Auffray , G. Auzinger , J. Baechler, D. Barney , A. Bermúdez Martínez , M. Bianco , B. Bilin , A.A. Bin Anuar , A. Bocci , C. Botta , E. Brondolin , C. Caillol , G. Cerminara , N. Chernyavskaya , D. d'Enterria , A. Dabrowski , A. David , A. De Roeck , M.M. Defranchis , M. Deile , M. Dobson , G. Franzoni , W. Funk , S. Giani, D. Gigi, K. Gill , F. Glege , L. Gouskos , J. Hegeman , J.K. Heikkilä , B. Huber, V. Innocente , T. James , P. Janot , O. Kaluzinska , S. Laurila , P. Lecoq , E. Leutgeb , C. Lourenço , L. Malgeri , M. Mannelli , A.C. Marini , M. Matthewman, A. Mehta , F. Meijers , S. Mersi , E. Meschi , V. Milosevic , F. Monti , F. Moortgat , M. Mulders , I. Neutelings , S. Orfanelli, F. Pantaleo , G. Petrucciani , A. Pfeiffer , M. Pierini , H. Qu , D. Rabady , B. Ribeiro Lopes , M. Rovere , H. Sakulin , S. Sanchez Cruz , S. Scarfi , C. Schwick, M. Selvaggi , A. Sharma , K. Shchelina , P. Silva , P. Sphicas ⁵⁷, A.G. Stahl Leiton , A. Steen , S. Summers , D. Treille , P. Tropea , D. Walter , J. Wanczyk ⁵⁸, J. Wang, S. Wuchterl , P. Zehetner , P. Zejdl , W.D. Zeuner

Paul Scherrer Institut, Villigen, Switzerland

T. Bevilacqua ⁵⁹, L. Caminada ⁵⁹, A. Ebrahimi , W. Erdmann , R. Horisberger , Q. Ingram , H.C. Kaestli , D. Kotlinski , C. Lange , M. Missiroli ⁵⁹, L. Noehre ⁵⁹, T. Rohe

ETH Zurich — Institute for Particle Physics and Astrophysics (IPA), Zurich, Switzerland

T.K. Arrestad , K. Androsov ⁵⁸, M. Backhaus , G. Bonomelli, A. Calandri , C. Cazzaniga , K. Datta , P. De Bryas Dexmiers D'archiac ⁵⁸, A. De Cosa , G. Dissertori , M. Dittmar, M. Donegà , F. Eble , M. Galli , K. Gedia , F. Glessgen , C. Grab , N. Härringer , T.G. Harte, D. Hits , W. Lustermann , A.-M. Lyon , R.A. Manzoni , M. Marchegiani , L. Marchese , C. Martin Perez , A. Mascellani ⁵⁸, F. Nessi-Tedaldi , F. Pauss , V. Perovic , S. Pigazzini , C. Reissel , T. Reitenspiess , B. Ristic , F. Riti , R. Seidita , J. Steggemann ⁵⁸, A. Tarabini , D. Valsecchi , R. Wallny

Universität Zürich, Zurich, Switzerland

C. Amsler^{ID}⁶⁰, P. Bärtschi^{ID}, M.F. Canelli^{ID}, K. Cormier^{ID}, M. Huwiler^{ID}, W. Jin^{ID}, A. Jofrehei^{ID}, B. Kilminster^{ID}, S. Leontsinis^{ID}, S.P. Liechti^{ID}, A. Macchiolo^{ID}, P. Meiring^{ID}, F. Meng^{ID}, U. Molinatti^{ID}, J. Motta^{ID}, A. Reimers^{ID}, P. Robmann, M. Senger^{ID}, E. Shokr, F. Stäger^{ID}, R. Tramontano^{ID}

National Central University, Chung-Li, Taiwan

C. Adloff⁶¹, D. Bhowmik, C.M. Kuo, W. Lin, P.K. Rout^{ID}, P.C. Tiwari^{ID}³⁸, S.S. Yu^{ID}

National Taiwan University (NTU), Taipei, Taiwan

L. Ceard, K.F. Chen^{ID}, P.s. Chen, Z.g. Chen, A. De Iorio^{ID}, W.-S. Hou^{ID}, T.h. Hsu, Y.w. Kao, S. Karmakar^{ID}, G. Kole^{ID}, Y.y. Li^{ID}, R.-S. Lu^{ID}, E. Paganis^{ID}, X.f. Su^{ID}, J. Thomas-Wilsker^{ID}, L.s. Tsai, H.y. Wu, E. Yazgan^{ID}

High Energy Physics Research Unit, Department of Physics, Faculty of Science, Chulalongkorn University, Bangkok, Thailand

C. Asawatangtrakuldee^{ID}, N. Srimanobhas^{ID}, V. Wachirapusanand^{ID}

Çukurova University, Physics Department, Science and Art Faculty, Adana, Turkey

D. Agyel^{ID}, F. Boran^{ID}, F. Dolek^{ID}, I. Dumanoglu^{ID}⁶², E. Eskut^{ID}, Y. Guler^{ID}⁶³, E. Gurpinar Guler^{ID}⁶³, C. Isik^{ID}, O. Kara, A. Kayis Topaksu^{ID}, U. Kiminsu^{ID}, G. Onengut^{ID}, K. Ozdemir^{ID}⁶⁴, A. Polatoz^{ID}, B. Tali^{ID}⁶⁵, U.G. Tok^{ID}, S. Turkcapar^{ID}, E. Uslan^{ID}, I.S. Zorbakir^{ID}

Middle East Technical University, Physics Department, Ankara, Turkey

G. Sokmen, M. Yalvac^{ID}⁶⁶

Bogazici University, Istanbul, Turkey

B. Akgun^{ID}, I.O. Atakisi^{ID}, E. Gülmez^{ID}, M. Kaya^{ID}⁶⁷, O. Kaya^{ID}⁶⁸, S. Tekten^{ID}⁶⁹

Istanbul Technical University, Istanbul, Turkey

A. Cakir^{ID}, K. Cankocak^{ID}^{62,70}, G.G. Dincer^{ID}⁶², Y. Komurcu^{ID}, S. Sen^{ID}⁷¹

Istanbul University, Istanbul, Turkey

O. Aydilek^{ID}⁷², V. Epshteyn^{ID}, B. Hacisahinoglu^{ID}, I. Hos^{ID}⁷³, B. Kaynak^{ID}, S. Ozkorucuklu^{ID}, O. Potok^{ID}, H. Sert^{ID}, C. Simsek^{ID}, C. Zorbilmez^{ID}

Yildiz Technical University, Istanbul, Turkey

S. Cerci^{ID}⁶⁵, B. Isildak^{ID}⁷⁴, D. Sunar Cerci^{ID}, T. Yetkin^{ID}

Institute for Scintillation Materials of National Academy of Science of Ukraine, Kharkiv, Ukraine

A. Boyaryntsev^{ID}, B. Grynyov^{ID}

National Science Centre, Kharkiv Institute of Physics and Technology, Kharkiv, Ukraine

L. Levchuk^{ID}

University of Bristol, Bristol, United Kingdom

D. Anthony , J.J. Brooke , A. Bundock , F. Bury , E. Clement , D. Cussans , H. Flacher , M. Glowacki , J. Goldstein , H.F. Heath , M.-L. Holmberg , L. Kreczko , S. Paramesvaran , L. Robertshaw , S. Seif El Nasr-Storey , V.J. Smith , N. Stylianou ⁷⁵, K. Walkingshaw Pass

Rutherford Appleton Laboratory, Didcot, United Kingdom

A.H. Ball , K.W. Bell , A. Belyaev ⁷⁶, C. Brew , R.M. Brown , D.J.A. Cockerill , C. Cooke , A. Elliot , K.V. Ellis , K. Harder , S. Harper , J. Linacre , K. Manolopoulos , D.M. Newbold , E. Olaiya , D. Petyt , T. Reis , A.R. Sahasransu , G. Salvi , T. Schuh , C.H. Shepherd-Themistocleous , I.R. Tomalin , K.C. Whalen , T. Williams

Imperial College, London, United Kingdom

R. Bainbridge , P. Bloch , C.E. Brown , O. Buchmuller , V. Cacchio , C.A. Carrillo Montoya , G.S. Chahal ⁷⁷, D. Colling , J.S. Dancu , I. Das , P. Dauncey , G. Davies , J. Davies , M. Della Negra , S. Fayer , G. Fedi , G. Hall , M.H. Hassanshahi , A. Howard , G. Illes , M. Knight , J. Langford , J. León Holgado , L. Lyons , A.-M. Magnan , S. Mallios , M. Mieskolainen , J. Nash ⁷⁸, M. Pesaresi , P.B. Pradeep , B.C. Radburn-Smith , A. Richards , A. Rose , K. Savva , C. Seez , R. Shukla , A. Tapper , K. Uchida , G.P. Uttley , L.H. Vage , T. Virdee ²⁹, M. Vojinovic , N. Wardle , D. Winterbottom

Brunel University, Uxbridge, United Kingdom

K. Coldham , J.E. Cole , A. Khan , P. Kyberd , I.D. Reid 

Baylor University, Waco, Texas, U.S.A.

S. Abdullin , A. Brinkerhoff , B. Caraway , E. Collins , J. Dittmann , K. Hatakeyama , J. Hiltbrand , B. McMaster , J. Samudio , S. Sawant , C. Sutantawibul , J. Wilson

Catholic University of America, Washington, DC, U.S.A.

R. Bartek , A. Dominguez , C. Huerta Escamilla , A.E. Simsek , R. Uniyal , A.M. Vargas Hernandez 

The University of Alabama, Tuscaloosa, Alabama, U.S.A.

B. Bam , A. Buchot Perraguin , R. Chudasama , S.I. Cooper , C. Crovella , S.V. Gleyzer , E. Pearson , C.U. Perez , P. Rumerio ⁷⁹, E. Usai , R. Yi

Boston University, Boston, Massachusetts, U.S.A.

A. Akpinar , C. Cosby , G. De Castro , Z. Demiragli , C. Erice , C. Fangmeier , C. Fernandez Madrazo , E. Fontanesi , D. Gastler , F. Golf , S. Jeon , J. O'cain , I. Reed , J. Rohlf , K. Salyer , D. Sperka , D. Spitzbart , I. Suarez , A. Tsatsos , A.G. Zecchinelli

Brown University, Providence, Rhode Island, U.S.A.

G. Benelli , X. Coubez ²⁵, D. Cutts , M. Hadley , U. Heintz , J.M. Hogan ⁸⁰, T. Kwon , G. Landsberg , K.T. Lau , D. Li , J. Luo , S. Mondal , M. Narain †, N. Pervan , S. Sagir ⁸¹, F. Simpson , M. Stamenkovic , N. Venkatasubramanian , X. Yan , W. Zhang

University of California, Davis, Davis, California, U.S.A.

S. Abbott , J. Bonilla , C. Brainerd , R. Breedon , H. Cai ,
 M. Calderon De La Barca Sanchez , M. Chertok , M. Citron , J. Conway , P.T. Cox ,
 R. Erbacher , F. Jensen , O. Kukral , G. Mocellin , M. Mulhearn , S. Ostrom , W. Wei ,
 Y. Yao , S. Yoo , F. Zhang

University of California, Los Angeles, California, U.S.A.

M. Bachtis , R. Cousins , A. Datta , G. Flores Avila, J. Hauser , M. Ignatenko , M.A. Iqbal ,
 T. Lam , E. Manca , A. Nunez Del Prado, D. Saltzberg , V. Valuev

University of California, Riverside, Riverside, California, U.S.A.

R. Clare , J.W. Gary , M. Gordon, G. Hanson , W. Si , S. Wimpenny †

University of California, San Diego, La Jolla, California, U.S.A.

A. Aportela, A. Arora , J.G. Branson , S. Cittolin , S. Cooperstein , D. Diaz , J. Duarte ,
 L. Giannini , Y. Gu, J. Guiang , R. Kansal , V. Krutelyov , R. Lee , J. Letts ,
 M. Masciovecchio , F. Mokhtar , S. Mukherjee , M. Pieri , M. Quinnan ,
 B.V. Sathia Narayanan , V. Sharma , M. Tadel , E. Vourliotis , F. Würthwein , Y. Xiang ,
 A. Yagil

University of California, Santa Barbara — Department of Physics, Santa Barbara, California, U.S.A.

A. Barzdukas , L. Brennan , C. Campagnari , K. Downham , C. Grieco , J. Incandela ,
 J. Kim , A.J. Li , P. Masterson , H. Mei , J. Richman , S.N. Santpur , U. Sarica ,
 R. Schmitz , F. Setti , J. Sheplock , D. Stuart , T.Á. Vámi , S. Wang , D. Zhang

California Institute of Technology, Pasadena, California, U.S.A.

A. Bornheim , O. Cerri, A. Latorre, J. Mao , H.B. Newman , G. Reales Gutiérrez,
 M. Spiropulu , J.R. Vlimant , C. Wang , S. Xie , R.Y. Zhu

Carnegie Mellon University, Pittsburgh, Pennsylvania, U.S.A.

J. Alison , S. An , M.B. Andrews , P. Bryant , M. Cremonesi, V. Dutta , T. Ferguson ,
 T.A. Gómez Espinosa , A. Harilal , A. Kallil Tharayil, C. Liu , T. Mudholkar , S. Murthy ,
 P. Palit , K. Park, M. Paulini , A. Roberts , A. Sanchez , W. Terrill

University of Colorado Boulder, Boulder, Colorado, U.S.A.

J.P. Cumalat , W.T. Ford , A. Hart , A. Hassani , G. Karathanasis , N. Manganelli ,
 J. Pearkes , A. Perloff , C. Savard , N. Schonbeck , K. Stenson , K.A. Ulmer ,
 S.R. Wagner , N. Zipper , D. Zuolo

Cornell University, Ithaca, New York, U.S.A.

J. Alexander , S. Bright-Thonney , X. Chen , D.J. Cranshaw , J. Fan , X. Fan , S. Hogan ,
 P. Kotamnives, J. Monroy , M. Oshiro , J.R. Patterson , M. Reid , A. Ryd , J. Thom ,
 P. Wittich , R. Zou

Fermi National Accelerator Laboratory, Batavia, Illinois, U.S.A.

M. Albrow , M. Alyari , O. Amram , G. Apollinari , A. Apresyan , L.A.T. Bauerick , D. Berry , J. Berryhill , P.C. Bhat , K. Burkett , J.N. Butler , A. Canepa , G.B. Cerati , H.W.K. Cheung , F. Chlebana , G. Cummings , J. Dickinson , I. Dutta , V.D. Elvira , Y. Feng , J. Freeman , A. Gandrakota , Z. Gecse , L. Gray , D. Green, A. Grummer , S. Grünendahl , D. Guerrero , O. Gutsche , R.M. Harris , R. Heller , T.C. Herwig , J. Hirschauer , B. Jayatilaka , S. Jindariani , M. Johnson , U. Joshi , T. Klijnsma , B. Klima , K.H.M. Kwok , S. Lammel , D. Lincoln , R. Lipton , T. Liu , C. Madrid , K. Maeshima , C. Mantilla , D. Mason , P. McBride , P. Merkel , S. Mrenna , S. Nahn , J. Ngadiuba , D. Noonan , S. Norberg, V. Papadimitriou , N. Pastika , K. Pedro , C. Pena ⁸², F. Ravera , A. Reinsvold Hall ⁸³, L. Ristori , M. Safdari , E. Sexton-Kennedy , N. Smith , A. Soha , L. Spiegel , S. Stoynev , J. Strait , L. Taylor , S. Tkaczyk , N.V. Tran , L. Uplegger , E.W. Vaandering , I. Zoi

University of Florida, Gainesville, Florida, U.S.A.

C. Aruta , P. Avery , D. Bourilkov , P. Chang , V. Cherepanov , R.D. Field, E. Koenig , M. Kolosova , J. Konigsberg , A. Korytov , K. Matchev , N. Menendez , G. Mitselmakher , K. Mohrman , A. Muthirakalayil Madhu , N. Rawal , S. Rosenzweig , Y. Takahashi , J. Wang 

Florida State University, Tallahassee, Florida, U.S.A.

T. Adams , A. Al Kadhim , A. Askew , S. Bower , R. Habibullah , V. Hagopian , R. Hashmi , R.S. Kim , S. Kim , T. Kolberg , G. Martinez, H. Prosper , P.R. Prova, M. Wulansatiti , R. Yohay , J. Zhang

Florida Institute of Technology, Melbourne, Florida, U.S.A.

B. Alsufyani, M.M. Baarmand , S. Butalla , S. Das , T. Elkafrawy ⁸⁴, M. Hohlmann , M. Rahmani, E. Yanes

University of Illinois Chicago, Chicago, U.S.A., Chicago, U.S.A.

M.R. Adams , A. Baty , C. Bennett, R. Cavanaugh , R. Escobar Franco , O. Evdokimov , C.E. Gerber , M. Hawksworth, A. Hingrajiya, D.J. Hofman , J.h. Lee , D. S. Lemos , A.H. Merrit , C. Mills , S. Nanda , G. Oh , B. Ozek , D. Pilipovic , R. Pradhan , E. Prifti, T. Roy , S. Rudrabhatla , M.B. Tonjes , N. Varelas , M.A. Wadud , Z. Ye , J. Yoo 

The University of Iowa, Iowa City, Iowa, U.S.A.

M. Alhusseini , D. Blend, K. Dilsiz ⁸⁵, L. Emediato , G. Karaman , O.K. Köseyan , J.-P. Merlo, A. Mestvirishvili ⁸⁶, O. Neogi, H. Ogul ⁸⁷, Y. Onel , A. Penzo , C. Snyder, E. Tiras 

Johns Hopkins University, Baltimore, Maryland, U.S.A.

B. Blumenfeld , L. Corcodilos , J. Davis , A.V. Gritsan , L. Kang , S. Kyriacou , P. Maksimovic , M. Roguljic , J. Roskes , S. Sekhar , M. Swartz 

The University of Kansas, Lawrence, Kansas, U.S.A.

A. Abreu , L.F. Alcerro Alcerro , J. Anguiano , S. Arteaga Escatel , P. Baringer , A. Bean , Z. Flowers , D. Grove , J. King , G. Krintiras , M. Lazarovits , C. Le Mahieu , J. Marquez , N. Minafra , M. Murray , M. Nickel , M. Pitt , S. Popescu ⁸⁹, C. Rogan , C. Royon , R. Salvatico , S. Sanders , C. Smith , G. Wilson

Kansas State University, Manhattan, Kansas, U.S.A.

B. Allmond , R. Gujju Gurunadha , A. Ivanov , K. Kaadze , Y. Maravin , J. Natoli , D. Roy , G. Sorrentino 

University of Maryland, College Park, Maryland, U.S.A.

A. Baden , A. Belloni , J. Bistany-riebman, Y.M. Chen , S.C. Eno , N.J. Hadley , S. Jabeen , R.G. Kellogg , T. Koeth , B. Kronheim, Y. Lai , S. Lascio , A.C. Mignerey , S. Nabili , C. Palmer , C. Papageorgakis , M.M. Paranjpe, L. Wang 

Massachusetts Institute of Technology, Cambridge, Massachusetts, U.S.A.

J. Bendavid , I.A. Cali , P.c. Chou , M. D'Alfonso , J. Eysermans , C. Freer , G. Gomez-Ceballos , M. Goncharov, G. Grossi, P. Harris, D. Hoang, D. Kovalevskyi , J. Krupa , L. Lavezzi , Y.-J. Lee , K. Long , C. McGinn, A. Novak , C. Paus , D. Rankin , C. Roland , G. Roland , S. Rothman , G.S.F. Stephans , Z. Wang , B. Wyslouch , T. J. Yang 

University of Minnesota, Minneapolis, Minnesota, U.S.A.

B. Crossman , B.M. Joshi , C. Kapsiak , M. Krohn , D. Mahon , J. Mans , B. Marzocchi , M. Revering , R. Rusack , R. Saradhy , N. Strobbe 

University of Mississippi, Oxford, Mississippi, U.S.A.

L.M. Cremaldi 

University of Nebraska-Lincoln, Lincoln, Nebraska, U.S.A.

K. Bloom , D.R. Claes , G. Haza , J. Hossain , C. Joo , I. Kravchenko , J.E. Siado , W. Tabb , A. Vagnerini , A. Wightman , F. Yan , D. Yu 

State University of New York at Buffalo, Buffalo, New York, U.S.A.

H. Bandyopadhyay , L. Hay , H.w. Hsia, I. Iashvili , A. Kalogeropoulos , A. Kharchilava , M. Morris , D. Nguyen , S. Rappoccio , H. Rejeb Sfar, A. Williams , P. Young 

Northeastern University, Boston, Massachusetts, U.S.A.

G. Alverson , E. Barberis , J. Dervan, Y. Haddad , Y. Han , A. Krishna , J. Li , M. Lu , G. Madigan , R. McCarthy , D.M. Morse , V. Nguyen , T. Orimoto , A. Parker , L. Skinnari , D. Wood 

Northwestern University, Evanston, Illinois, U.S.A.

J. Bueghly, S. Dittmer , K.A. Hahn , Y. Liu , Y. Miao , D.G. Monk , M.H. Schmitt , A. Taliercio , M. Velasco

University of Notre Dame, Notre Dame, Indiana, U.S.A.

G. Agarwal , R. Band , R. Bucci, S. Castells , A. Das , R. Goldouzian , M. Hildreth , K.W. Ho , K. Hurtado Anampa , T. Ivanov , C. Jessop , K. Lannon , J. Lawrence , N. Loukas , L. Lutton , J. Mariano, N. Marinelli, I. Mcalister, T. McCauley , C. Mcgrady , C. Moore , Y. Musienko ¹⁷, H. Nelson , M. Osherson , A. Piccinelli , R. Ruchti , A. Townsend , Y. Wan, M. Wayne , H. Yockey, M. Zarucki , L. Zygala

The Ohio State University, Columbus, Ohio, U.S.A.

A. Basnet , B. Bylsma, M. Carrigan , L.S. Durkin , C. Hill , M. Joyce , M. Nunez Ornelas , K. Wei, B.L. Winer , B. R. Yates 

Princeton University, Princeton, New Jersey, U.S.A.

H. Bouchamaoui , P. Das , G. Dezoort , P. Elmer , A. Frankenthal , B. Greenberg , N. Haubrich , K. Kennedy, G. Kopp , S. Kwan , D. Lange , A. Loeliger , D. Marlow , I. Ojalvo , J. Olsen , A. Shevelev , D. Stickland , C. Tully

University of Puerto Rico, Mayaguez, Puerto Rico, U.S.A.

G. Fidalgo , S. Malik , C. Suarez

Purdue University, West Lafayette, Indiana, U.S.A.

A.S. Bakshi , V.E. Barnes , S. Chandra , R. Chawla , A. Gu , L. Gutay, M. Jones , A.W. Jung , A.M. Koshy, M. Liu , G. Negro , N. Neumeister , G. Paspalaki , S. Piperov , V. Scheurer, J.F. Schulte , M. Stojanovic , J. Thieman , A. K. Virdi , F. Wang , W. Xie

Purdue University Northwest, Hammond, Indiana, U.S.A.

J. Dolen , N. Parashar , A. Pathak 

Rice University, Houston, Texas, U.S.A.

D. Acosta , T. Carnahan , K.M. Ecklund , P.J. Fernández Manteca , S. Freed, P. Gardner, F.J.M. Geurts , W. Li , J. Lin , O. Miguel Colin , B.P. Padley , R. Redjimi, J. Rotter , E. Yigitbasi , Y. Zhang 

University of Rochester, Rochester, New York, U.S.A.

A. Bodek , P. de Barbaro , R. Demina , J.L. Dulemba , A. Garcia-Bellido , O. Hindrichs , A. Khukhunaishvili , N. Parmar, P. Parygin ⁹⁰, E. Popova ⁹⁰, R. Taus 

The Rockefeller University, New York, New York, U.S.A.

K. Goulianatos 

Rutgers, The State University of New Jersey, Piscataway, New Jersey, U.S.A.

B. Chiarito, J.P. Chou , S.V. Clark , D. Gadkari , Y. Gershtein , E. Halkiadakis , M. Heindl , C. Houghton , D. Jaroslawski , O. Karacheban ²⁷, S. Konstantinou , I. Laflotte , A. Lath , R. Montalvo, K. Nash, J. Reichert , H. Routray , P. Saha , S. Salur , S. Schnetzer, S. Somalwar , R. Stone , S.A. Thayil , S. Thomas, J. Vora , H. Wang

University of Tennessee, Knoxville, Tennessee, U.S.A.

H. Acharya, D. Ally^{id}, A.G. Delannoy^{id}, S. Fiorendi^{id}, S. Higginbotham^{id}, T. Holmes^{id},
A.R. Kanuganti^{id}, N. Karunaratna^{id}, L. Lee^{id}, E. Nibigira^{id}, S. Spanier^{id}

Texas A&M University, College Station, Texas, U.S.A.

D. Aebi^{id}, M. Ahmad^{id}, T. Akhter^{id}, O. Bouhalil^{id}⁹¹, R. Eusebi^{id}, J. Gilmore^{id}, T. Huang^{id},
T. Kamon^{id}⁹², H. Kim^{id}, S. Luo^{id}, R. Mueller^{id}, D. Overton^{id}, D. Rathjens^{id}, A. Safonov^{id}

Texas Tech University, Lubbock, Texas, U.S.A.

N. Akchurin^{id}, J. Damgov^{id}, N. Gogate^{id}, V. Hegde^{id}, A. Hussain^{id}, Y. Kazhykarim,
K. Lamichhane^{id}, S.W. Lee^{id}, A. Mankel^{id}, T. Peltola^{id}, I. Volobouev^{id}

Vanderbilt University, Nashville, Tennessee, U.S.A.

E. Appelt^{id}, Y. Chen^{id}, S. Greene, A. Gurrola^{id}, W. Johns^{id}, R. Kunawalkam Elayavalli^{id},
A. Melo^{id}, F. Romeo^{id}, P. Sheldon^{id}, S. Tuo^{id}, J. Velkovska^{id}, J. Viinikainen^{id}

University of Virginia, Charlottesville, Virginia, U.S.A.

B. Cardwell^{id}, B. Cox^{id}, J. Hakala^{id}, R. Hirosky^{id}, A. Ledovskoy^{id}, C. Neu^{id}

Wayne State University, Detroit, Michigan, U.S.A.

S. Bhattacharya^{id}, P.E. Karchin^{id}

University of Wisconsin — Madison, Madison, Wisconsin, U.S.A.

A. Aravind, S. Banerjee^{id}, K. Black^{id}, T. Bose^{id}, S. Dasu^{id}, I. De Bruyn^{id}, P. Everaerts^{id},
C. Galloni, H. He^{id}, M. Herndon^{id}, A. Herve^{id}, C.K. Koraka^{id}, A. Lanaro, R. Loveless^{id},
J. Madhusudanan Sreekala^{id}, A. Mallampalli^{id}, A. Mohammadi^{id}, S. Mondal, G. Parida^{id},
L. Pétré^{id}, D. Pinna, A. Savin, V. Shang^{id}, V. Sharma^{id}, W.H. Smith^{id}, D. Teague, H.F. Tsoi^{id},
W. Vetens^{id}, A. Warden^{id}

Authors affiliated with an institute or an international laboratory covered by a cooperation agreement with CERN

S. Afanasiev^{id}, V. Alexakhin^{id}, V. Andreev^{id}, Yu. Andreev^{id}, T. Aushev^{id}, M. Azarkin^{id},
A. Babaev^{id}, V. Blinov⁹³, E. Boos^{id}, V. Borshch^{id}, D. Budkouski^{id}, V. Bunichev^{id},
M. Chadeeva^{id}⁹³, V. Chekhovsky, R. Chistov^{id}⁹³, A. Dermenev^{id}, T. Dimova^{id}⁹³, D. Druzhkin^{id}⁹⁴,
M. Dubinin^{id}⁸², L. Dudko^{id}, A. Ershov^{id}, G. Gavrilov^{id}, V. Gavrilov^{id}, S. Gninenko^{id},
V. Golovtcov^{id}, N. Golubev^{id}, I. Golutvin^{id}, I. Gorbunov^{id}, A. Gribushin^{id}, Y. Ivanov^{id},
V. Kachanov^{id}, V. Karjavine^{id}, A. Karneyeu^{id}, V. Kim^{id}⁹³, M. Kirakosyan, D. Kirpichnikov^{id},
M. Kirsanov^{id}, V. Klyukhin^{id}, O. Kodolova^{id}⁹⁵, D. Konstantinov^{id}, V. Korenkov^{id}, A. Kozyrev^{id}⁹³,
N. Krasnikov^{id}, A. Lanev^{id}, P. Levchenko^{id}⁹⁶, N. Lychkovskaya^{id}, V. Makarenko^{id},
A. Malakhov^{id}, V. Matveev^{id}⁹³, V. Murzin^{id}, A. Nikitenko^{id}^{97,95}, S. Obraztsov^{id}, V. Oreshkin^{id},
V. Palichik^{id}, V. Perelygin^{id}, S. Petrushanko^{id}, S. Polikarpov^{id}⁹³, V. Popov^{id}, O. Radchenko^{id}⁹³,
M. Savina^{id}, V. Savrin^{id}, V. Shalaev^{id}, S. Shmatov^{id}, S. Shulha^{id}, Y. Skoppen^{id}⁹³,
S. Slabospitskii^{id}, V. Smirnov^{id}, A. Snigirev^{id}, D. Sosnov^{id}, V. Sulimov^{id}, E. Tcherniaev^{id},
A. Terkulov^{id}, O. Teryaev^{id}, I. Tlisova^{id}, A. Toropin^{id}, L. Uvarov^{id}, A. Uzunian^{id}, A. Vorobyev[†],
N. Voytishin^{id}, B.S. Yuldashev⁹⁸, A. Zarubin^{id}, I. Zhizhin^{id}, A. Zhokin^{id}

[†] Deceased

¹ Also at Yerevan State University, Yerevan, Armenia

² Also at TU Wien, Vienna, Austria

³ Also at Institute of Basic and Applied Sciences, Faculty of Engineering, Arab Academy for Science, Technology and Maritime Transport, Alexandria, Egypt

⁴ Also at Ghent University, Ghent, Belgium

⁵ Also at Universidade do Estado do Rio de Janeiro, Rio de Janeiro, Brazil

⁶ Also at Universidade Estadual de Campinas, Campinas, Brazil

⁷ Also at Federal University of Rio Grande do Sul, Porto Alegre, Brazil

⁸ Also at UFMS, Nova Andradina, Brazil

⁹ Also at Nanjing Normal University, Nanjing, China

¹⁰ Now at The University of Iowa, Iowa City, Iowa, U.S.A.

¹¹ Also at University of Chinese Academy of Sciences, Beijing, China

¹² Also at China Center of Advanced Science and Technology, Beijing, China

¹³ Also at University of Chinese Academy of Sciences, Beijing, China

¹⁴ Also at China Spallation Neutron Source, Guangdong, China

¹⁵ Now at Henan Normal University, Xinxiang, China

¹⁶ Also at Université Libre de Bruxelles, Bruxelles, Belgium

¹⁷ Also at an institute or an international laboratory covered by a cooperation agreement with CERN

¹⁸ Also at Suez University, Suez, Egypt

¹⁹ Now at British University in Egypt, Cairo, Egypt

²⁰ Also at Purdue University, West Lafayette, Indiana, U.S.A.

²¹ Also at Université de Haute Alsace, Mulhouse, France

²² Also at Department of Physics, Tsinghua University, Beijing, China

²³ Also at The University of the State of Amazonas, Manaus, Brazil

²⁴ Also at University of Hamburg, Hamburg, Germany

²⁵ Also at RWTH Aachen University, III. Physikalisches Institut A, Aachen, Germany

²⁶ Also at Bergische University Wuppertal (BUW), Wuppertal, Germany

²⁷ Also at Brandenburg University of Technology, Cottbus, Germany

²⁸ Also at Forschungszentrum Jülich, Juelich, Germany

²⁹ Also at CERN, European Organization for Nuclear Research, Geneva, Switzerland

³⁰ Also at Institute of Physics, University of Debrecen, Debrecen, Hungary

³¹ Also at Institute of Nuclear Research ATOMKI, Debrecen, Hungary

³² Now at Universitatea Babes-Bolyai — Facultatea de Fizica, Cluj-Napoca, Romania

³³ Also at MTA-ELTE Lendület CMS Particle and Nuclear Physics Group, Eötvös Loránd University, Budapest, Hungary

³⁴ Also at HUN-REN Wigner Research Centre for Physics, Budapest, Hungary

³⁵ Also at Physics Department, Faculty of Science, Assiut University, Assiut, Egypt

³⁶ Also at Punjab Agricultural University, Ludhiana, India

³⁷ Also at University of Visva-Bharati, Santiniketan, India

³⁸ Also at Indian Institute of Science (IISc), Bangalore, India

³⁹ Also at IIT Bhubaneswar, Bhubaneswar, India

⁴⁰ Also at Institute of Physics, Bhubaneswar, India

⁴¹ Also at University of Hyderabad, Hyderabad, India

⁴² Also at Deutsches Elektronen-Synchrotron, Hamburg, Germany

⁴³ Also at Isfahan University of Technology, Isfahan, Iran

⁴⁴ Also at Sharif University of Technology, Tehran, Iran

⁴⁵ Also at Department of Physics, University of Science and Technology of Mazandaran, Behshahr, Iran

⁴⁶ Also at Department of Physics, Isfahan University of Technology, Isfahan, Iran

⁴⁷ Also at Italian National Agency for New Technologies, Energy and Sustainable Economic Development, Bologna, Italy

⁴⁸ Also at Centro Siciliano di Fisica Nucleare e di Struttura Della Materia, Catania, Italy

⁴⁹ Also at Università degli Studi Guglielmo Marconi, Roma, Italy

- ⁵⁰ Also at Scuola Superiore Meridionale, Università di Napoli ‘Federico II’, Napoli, Italy
⁵¹ Also at Fermi National Accelerator Laboratory, Batavia, Illinois, U.S.A.
⁵² Also at Consiglio Nazionale delle Ricerche — Istituto Officina dei Materiali, Perugia, Italy
⁵³ Also at Department of Applied Physics, Faculty of Science and Technology, Universiti Kebangsaan Malaysia, Bangi, Malaysia
⁵⁴ Also at Consejo Nacional de Ciencia y Tecnología, Mexico City, Mexico
⁵⁵ Also at Trincomalee Campus, Eastern University, Sri Lanka, Nilaveli, Sri Lanka
⁵⁶ Also at Saegis Campus, Nugegoda, Sri Lanka
⁵⁷ Also at National and Kapodistrian University of Athens, Athens, Greece
⁵⁸ Also at Ecole Polytechnique Fédérale Lausanne, Lausanne, Switzerland
⁵⁹ Also at Universität Zürich, Zurich, Switzerland
⁶⁰ Also at Stefan Meyer Institute for Subatomic Physics, Vienna, Austria
⁶¹ Also at Laboratoire d’Annecy-le-Vieux de Physique des Particules, IN2P3-CNRS, Annecy-le-Vieux, France
⁶² Also at Near East University, Research Center of Experimental Health Science, Mersin, Turkey
⁶³ Also at Konya Technical University, Konya, Turkey
⁶⁴ Also at Izmir Bakircay University, Izmir, Turkey
⁶⁵ Also at Adiyaman University, Adiyaman, Turkey
⁶⁶ Also at Bozok Üniversitesi Rektörlüğü, Yozgat, Turkey
⁶⁷ Also at Marmara University, Istanbul, Turkey
⁶⁸ Also at Milli Savunma University, Istanbul, Turkey
⁶⁹ Also at Kafkas University, Kars, Turkey
⁷⁰ Now at stanbul Okan University, Istanbul, Turkey
⁷¹ Also at Hacettepe University, Ankara, Turkey
⁷² Also at Erzincan Binali Yıldırım University, Erzincan, Turkey
⁷³ Also at Istanbul University — Cerrahpasa, Faculty of Engineering, Istanbul, Turkey
⁷⁴ Also at Yildiz Technical University, Istanbul, Turkey
⁷⁵ Also at Vrije Universiteit Brussel, Brussel, Belgium
⁷⁶ Also at School of Physics and Astronomy, University of Southampton, Southampton, United Kingdom
⁷⁷ Also at IPPP Durham University, Durham, United Kingdom
⁷⁸ Also at Monash University, Faculty of Science, Clayton, Australia
⁷⁹ Also at Università di Torino, Torino, Italy
⁸⁰ Also at Bethel University, St. Paul, Minnesota, U.S.A.
⁸¹ Also at Karamanoğlu Mehmetbey University, Karaman, Turkey
⁸² Also at California Institute of Technology, Pasadena, California, U.S.A.
⁸³ Also at United States Naval Academy, Annapolis, Maryland, U.S.A.
⁸⁴ Also at Ain Shams University, Cairo, Egypt
⁸⁵ Also at Bingöl University, Bingöl, Turkey
⁸⁶ Also at Georgian Technical University, Tbilisi, Georgia
⁸⁷ Also at Sinop University, Sinop, Turkey
⁸⁸ Also at Erciyes University, Kayseri, Turkey
⁸⁹ Also at Horia Hulubei National Institute of Physics and Nuclear Engineering (IFIN-HH), Bucharest, Romania
⁹⁰ Now at an institute or an international laboratory covered by a cooperation agreement with CERN
⁹¹ Also at Texas A&M University at Qatar, Doha, Qatar
⁹² Also at Kyungpook National University, Daegu, Korea
⁹³ Also at another institute or international laboratory covered by a cooperation agreement with CERN
⁹⁴ Also at Universiteit Antwerpen, Antwerpen, Belgium
⁹⁵ Also at Yerevan Physics Institute, Yerevan, Armenia
⁹⁶ Also at Northeastern University, Boston, Massachusetts, U.S.A.
⁹⁷ Also at Imperial College, London, United Kingdom
⁹⁸ Also at Institute of Nuclear Physics of the Uzbekistan Academy of Sciences, Tashkent, Uzbekistan